

2

CUMENTATION PAGE

Form Approved  
OMB No. 0704-0188

AD-A211 002 **TC**

1b RESTRICTIVE MARKINGS

2b. DECLASSIFICATION/DOWNGRADING SCHEDULE  
UNCLASSIFIED 8 1989

CTE

3 DISTRIBUTION/AVAILABILITY OF REPORT  
Approved for public release: distribution unlimited.

4. PERFORMING ORGANIZATION REPORT NUMBER(S)  
C3086-FR-001a

**D** **CS**

5. MONITORING ORGANIZATION REPORT NUMBER(S)  
R&D 5970-MS-01

6a. NAME OF PERFORMING ORGANIZATION  
Cambridge Consultants Ltd

6b. OFFICE SYMBOL  
(If applicable)

7a. NAME OF MONITORING ORGANIZATION  
European Research Office  
USARDSG-UK

5c. ADDRESS (City, State, and ZIP Code)  
Science Park, Milton Road,  
Cambridge, CB4 4DW. UK

7b. ADDRESS (City, State, and ZIP Code)  
PO Box 65  
FPO NY 09510-1500

8a. NAME OF FUNDING/SPONSORING ORGANIZATION  
European Research Office  
USARDSG-UK

8b. OFFICE SYMBOL  
(If applicable)  
AMXSN-UK-RP

9 PROCUREMENT INSTRUMENT IDENTIFICATION NUMBER  
DAJA45-88-C-0014

8c. ADDRESS (City, State, and ZIP Code)  
PO Box 55  
FPO NY 09510-1500

10 SOURCE OF FUNDING NUMBERS

PROGRAM ELEMENT NO.	PROJECT NO.	TASK NO.	WORK UNIT ACCESSION NO.
61103A	1161103 BH07	05	

1. TITLE (Include Security Classification)  
Custom Diffraction Gratings

2. PERSONAL AUTHOR(S)  
T R Empson

13a. TYPE OF REPORT  
Final

13b. TIME COVERED  
FROM April 85 to April 89

14. DATE OF REPORT (Year, Month, Day)  
1989-7-7

15. PAGE COUNT  
35

5. SUPPLEMENTARY NOTATION

COSATI CODES		
FIELD	GROUP	SUB-GROUP
2005		

18 SUBJECT TERMS (Continue on reverse if necessary and identify by block number)  
Optics, grating, deflection; laser

1. ABSTRACT (Continue on reverse if necessary and identify by block number)

The objective of this work was to design, develop and manufacture a batch of custom transmission diffraction gratings with a low zero-order optical transmission across the visible and near-infrared waveband. A high laser damage threshold was also desirable. It was shown that neither conventional blazed gratings nor holographically-fabricated sinusoidal photoresist gratings were entirely suitable. The preferred approach was to use reactive ion etching to transfer a quasi-sinusoidal groove profile into the surface of a "hard" substrate such as fused silica. Differential etch rates were exploited to achieve a larger groove amplitude in the etched grating than in the photoresist "mask".

Of the batch of ten gratings which was supplied, the best grating exhibited a zero-order transmission which did not exceed 6% over the wavelength range 543nm - 875nm. The main conclusion of the work was that a deep-grooved surface relief transmission diffraction grating can provide a broad-band optical attenuation of around 95% across the visible and near-infrared waveband. The use of reactive ion etching techniques can enable the production of such gratings with high laser damage thresholds.

20. DISTRIBUTION/AVAILABILITY OF ABSTRACT  
 UNCLASSIFIED/UNLIMITED  SAME AS RPT  DTIC USERS

21. ABSTRACT SECURITY CLASSIFICATION  
UNCLASSIFIED

8. NAME OF RESPONSIBLE INDIVIDUAL  
Dr W C Simmons

22b. TELEPHONE (Include Area Code)  
01 409 4423

22c. OFFICE SYMBOL  
AMXSN-UK-RM

89 8 07 069

CUSTOM DIFFRACTION GRATINGS

T R Empson  
Cambridge Consultants Limited  
Science Park  
Milton Road  
CAMBRIDGE  
CB4 4DW  
United Kingdom

Contract No: DAJA45-88-C-0014

FINAL REPORT  
April 1988 - April 1989

Date of Report: 7 July 1989

Approved	✓
Reviewed	
Checked	
By	
Date	
Initials	
Signature	
Stamp	
Other	

A-1

The Research reported in this document has been made possible through the support and sponsorship of the US Government through its European Research Office of the US Army. This report is intended only for the internal management use of the Contractor and the US Government.

Cambridge Consultants Ltd

C O N T E N T S

	<u>Page No</u>
SUMMARY	2
1 INTRODUCTION	4
2 BLAZED GRATINGS	5
2.1 Introduction	5
2.2 Target Specification	5
2.3 Theory of Blazed Gratings	6
2.4 Grating Materials	7
2.5 Blaze Efficiency	8
2.6 Fabrication of Blazed Gratings	9
3 GRATINGS WITH SYMMETRICAL GROOVE PROFILES	12
3.1 Introduction	12
3.2 Sinusoidal Gratings	12
3.3 Non-Sinusoidal Gratings	15
3.4 Fabrication of Symmetrical Gratings	16
4 CONCLUSIONS AND RECOMMENDATIONS	21
4.1 Conclusions	21
4.2 Recommendations	22

REFERENCES

FIGURES

Appendix A: Commercial Blazed Transmission Gratings

Appendix B: NPL Report

Appendix C: Grating Specifications

## SUMMARY

This Report describes a programme of work carried out on behalf of the US Army Research Development and Standardisation Group by Cambridge Consultants Limited. The objective was to design, develop and manufacture a custom transmission diffraction grating with specific optical characteristics. The prime requirement was that the grating should exhibit a low zero-order optical transmission across the visible and near-infrared waveband. It was also desirable that the grating should have a high laser damage threshold.

The development work carried out by Cambridge Consultants showed first that it was impractical to attempt to meet the requirement with a conventional blazed grating because of major fabrication problems associated with the very large groove angle which would be needed. Next, it was established that a transmission grating with a sinusoidal groove profile could in principle achieve the desired performance. Such gratings are normally fabricated in photoresist using an interferometric technique, but such gratings generally have low laser damage thresholds. Moreover, the required groove amplitude was somewhat larger than can be easily achieved using the interferometric technique. For these reasons, the preferred grating fabrication approach which was finally adopted was to use reactive ion etching to transfer a quasi-sinusoidal groove profile into the surface of a "hard" substrate such as fused silica. Differential etch rates were exploited to achieve a larger groove amplitude in the etched grating than in the photoresist "mask".

A total of seven custom gratings were supplied during the course of the Contract, plus three commercial gratings procured by Cambridge Consultants on behalf of USARDSG. The best of the custom gratings exhibited a zero-order transmission which did not exceed 6% over the wavelength range 543nm-875nm. This result was in reasonably good agreement with a theoretical analysis of the zero-order transmission characteristics of surface relief gratings based upon work published by M T Gale [8].

Cambridge Consultants Ltd

C3086-FR-001a

The main conclusion of the work was that a deep-grooved surface relief transmission diffraction grating can provide a broad-band optical attenuation of around 95% across the visible and near-infrared waveband. The use of reactive ion etching techniques can enable the production of such gratings with high laser damage thresholds. Higher levels of attenuation can probably be achieved by the use of a "crossed" grating structure (two gratings superimposed at right angles to each other).

It is recommended that future work should concentrate first on optimising process parameters so that etched gratings with controlled groove amplitude and profile may be made in a reliable and repeatable fashion, using substrates of representative size and material. Some suggestions are also presented for the development of a fast optical "switch" which combines a hard crossed grating with a "non-linear" polymer layer. With such a device, the grating would remain inoperative under normal conditions of illumination, but would "turn on" rapidly when a high-energy laser pulse was received. A preliminary analysis suggests that such a device could have a activation energy in the range 1-10 $\mu$ J, and a broad-band optical density when activated of up to 2.5.

1 INTRODUCTION

The US Army Research, Development and Standardisation Group (hereinafter "USARDSG") is currently sponsoring a research programme at the School of Electronic Engineering Science, University College of North Wales ("UCNW"). As part of this work, a requirement has emerged for a non-standard optical device, namely a transmission diffraction grating with specific optical characteristics. Cambridge Consultants Limited ("CCL") offer a service for the design, development and fabrication of custom diffractive optical elements, and have recently completed a three-phase programme of work, sponsored by USARDSG, to provide gratings suitable for UCNW's research requirements.

## 2 BLAZED GRATINGS

### 2.1 Introduction

The eventual intended application of diffraction gratings such as those under consideration during this Contract is as protection devices against high-power and/or high-energy lasers in the VNIR (visible and near-infrared) region of the spectrum. In general, when a diffraction grating of pitch  $d$  is illuminated (at normal incidence, say) by a beam of radiation of wavelength  $\lambda$ , the energy of the incident beam will be redistributed between an undiffracted "zero-order" beam and one or more diffracted beams, as long as  $\lambda < d$ . A number of different types of diffraction grating exist; in the present Contract, we are concerned only with transmission phase gratings. The distinction between transmission and reflection gratings is self-evident: in the VNIR region, transmission gratings are normally all-dielectric devices, while reflection gratings (which are much more commonly used) usually have a metallic coating which greatly enhances their diffraction efficiency. Gratings which generate diffracted orders by modulating the amplitude, as opposed to the phase, of the incoming radiation are not suitable for applications (such as the present one) in which diffraction efficiency is an important consideration.

### 2.2 Target Specification

At the beginning of the Contract, UCNW provided the following target specification for the particular transmission phase grating which they required.

Frequency :  $600\text{mm}^{-1}$   
Blaze angle :  $27^\circ$   
Area :  $30\text{mm} \times 30\text{mm}$   
Operating waveband :  $0.4 - 1.06\mu\text{m}$

It was also stated that particular emphasis should be placed upon the  $0.4\mu\text{m}$  to  $0.8\mu\text{m}$  region of the operating waveband. The blaze angle of  $27^\circ$

was specified as being that which would give optimum blaze performance at a wavelength of 0.55 $\mu$ m.

### 2.3 Theory of Blazed Gratings

Consider Figure 1, which shows the general case of a blazed transmission diffraction grating composed of a material of refractive index  $n_g$ , attached to a substrate of index  $n_s$ . We consider the case where light is incident normally upon the non-grating side of the substrate. The groove angle is  $\theta$  and the first-order diffraction angle is  $\beta$ .  $d$  is the grating pitch and the optical wavelength. Since in the analysis of a simple blazed grating we are entirely concerned with first-order diffracted beams, the order of diffraction (usually called  $m$ ) is set at unity throughout. So, the familiar diffraction grating equation becomes

$$d \sin \beta = \lambda \quad (1)$$

At the grating facets, Snell's law gives

$$n_g \sin \theta = \sin (\theta + \beta) \quad (2)$$

Equations (1) and (2) may be combined to obtain an expression for the groove angle  $\theta$  needed for the grating to be blazed for a given blaze wavelength  $\lambda_b$ :

$$\theta = \tan^{-1}[\lambda_b / (n_g d - [d^2 - \lambda_b^2]^{0.5})] \quad (3)$$

At these values of  $\theta$  and  $\lambda_b$ , both diffraction across a multiplicity of grating grooves, and refraction at each individual groove facet, give rise to a beam propagating at the same angle  $\beta$ . This reinforcement of diffraction by refraction is the mechanism by which in a blazed grating, a large proportion of the incident radiation is diffracted into one of the two first order beams.

If we now put  $d = 1.67\mu\text{m}$  ( $=1/600\text{mm}$ ),  $n_g = 1.6$  and  $\lambda_b = 550\text{nm}$  in equation (3), we obtain  $\theta = 26.7^\circ$ . The slight discrepancy between this value and the  $27^\circ$  specified was explained by the fact that UCNW used values of  $d = 2\mu\text{m}$  (i.e. grating period  $500\text{mm}^{-1}$ ) and  $n_g = 1.5$  to derive a value of  $\theta = 27.0^\circ$ . The corresponding angles of diffraction  $\beta$  at  $550\text{nm}$  are  $19.3^\circ$  (for a  $600\text{mm}^{-1}$  grating) and  $16.0^\circ$  (for a  $500\text{mm}^{-1}$  grating). These angles of diffraction are significant in that UCNW indicated that  $\beta_{\text{min}}$ , i.e. the value of  $\beta$  at  $\lambda = 400\text{nm}$ , should be  $13^\circ$  or more to ensure adequate spatial separation between the zero-order and first-order beams. For a  $600\text{mm}^{-1}$  grating,  $\beta_{\text{min}} = 13.9^\circ$  ( $\beta_{\text{min}} = 11.5^\circ$  for a  $500\text{mm}^{-1}$  grating).

#### 2.4 Grating Materials

The calculations above illustrate the significance of the grating material. For the present application, there are essentially three possible materials. First, most commercially-available gratings are cast replicas of ruled gratings. The casting process results in a grating with the grooves formed in a very thin layer of clear epoxy resin which adheres strongly to the surface of the substrate, which will normally be optical glass (e.g. Schott type BK7) for transmission gratings. In this case, the grating refractive index  $n_g$ , i.e. the index of the epoxy resin, is about 1.59 at  $550\text{nm}$ .

The second possible grating type is a custom holographic grating. In this case, the grating is formed as a surface relief structure in a thin layer of photoresist (usually Shipley AZ1350), again supported on an optical glass substrate. In this case, the grating index is approximately 1.6 in the mid-visible.

The third possible type of grating is one in which the surface relief structure mentioned above is transferred into the substrate by either ion- or plasma-etching. In this case, the final grating exists directly on the surface of the substrate, so that the grating index is equal to the substrate index. For a standard optical glass such as Schott BK7, the index at  $550\text{nm}$  is 1.52. Alternatively, a material whose etching behaviour

is well-characterised, such as Spectrosil-B (a type of synthetic fused silica) may be preferred. In this case, the index at 550nm is 1.46.

These various grating materials are listed in Table 1, which also shows the refractive index at 550nm, the theoretical groove angle (for a pitch of  $600\text{mm}^{-1}$  and blaze wavelength of 550nm), the corresponding groove depth  $a'$  ( $a' = d\sin\theta\cos\theta$ ), and the critical groove angle  $\theta_{\text{max}}$  ( $\theta_{\text{max}} = \sin^{-1}(1/n_g)$ ). For diffraction angles greater than  $\theta_{\text{max}}$ , the incident light will undergo total internal reflection at the groove facets, and very little light will emerge from the grating.

Grating Material	$n_{550}$	Groove Angle	Groove Depth/ $\mu\text{m}$	$\theta_{\text{max}}$
Spectrosil-B	1.46	32.6°	0.76	43.2°
Schott BK7	1.57	29.8°	0.72	41.1°
Epoxy resin	1.59	27.1°	0.68	40.0°
AZ1350 photoresist	1.60	26.7°	0.67	38.7°

TABLE 1

### 2.5 Blaze Efficiency

The word "theoretical" was underlined in the last paragraph of Section 2.4. This is because the agreement between blaze wavelength as determined from equation (3) (for fixed  $\theta$ ) and as measured experimentally is not always close. In particular, the theory presented in Section 2.3, which is based solely on geometrical optics considerations, breaks down as the grating period approaches the operating wavelength. Even with a  $600\text{mm}^{-1}$  grating, quite marked discrepancies can be observed.

For example, consider two standard gratings manufactured by Milton Roy. The specifications are as follows:

- (1) Catalogue no. 35-54-08-550: 600 grooves/mm: groove angle 28.7°
- (2) Catalogue no. 35-54-08-660: 600 grooves/mm: groove angle 34°

Combining equations (1) and (2), we obtain the following expression for the blaze wavelength  $\lambda_b$ :

$$\lambda_b = d \sin[\sin^{-1}(n_g \sin \theta) - \theta] \quad (4)$$

For gratings (1) and (2), equation (4) gives values of  $\lambda_b$  of 599nm and 802nm respectively. However, when the efficiencies  $\eta$  of these two gratings are measured, the results are as shown in Figure 2. The graphs show peak efficiencies at about 480nm and 670nm respectively.

So, the observations noted above suggest that the deviation from the geometrical theory of blazing manifests itself as a shift of  $\lambda_b$  to a shorter wavelength than predicted. Therefore, if peak grating efficiency is required at 550nm, it may be prudent to aim for a groove angle rather larger than the figure (for a given grating material) shown in Table 1, while bearing in mind the requirement not to exceed  $\theta_{max}$ .

## 2.6 Fabrication of Blazed Gratings

There are essentially two main ways of making custom blazed transmission gratings. The first way involves the creation of a blazed surface relief profile in photoresist, and a number of techniques have been described for doing this. The second way involves the use of a photoresist mask (which may or may not have a blazed profile) in a dry-etching process which results in the formation of a blazed profile on the surface of the underlying substrate. The latter technique results in a device whose laser damage and thermal characteristics are essentially those of the substrate material, and furthermore one which can be cleaned when necessary with any of the standard optical cleaning solvents, e.g. acetone, propanol etc.

For these reasons, these dry-etched gratings have been called "hard" gratings, as opposed to the photoresist gratings which have been called "soft" gratings. The laser damage and thermal characteristics of soft gratings are essentially those of the photoresist itself, and photoresist is generally much less robust than substrate materials such as glass and silica. It is also soluble in most organic solvents, so that soft gratings cannot easily be cleaned.

#### 2.6.1 Soft Gratings

Techniques for making blazed photoresist gratings are described by Hutley [1]. Unfortunately, most of them are designed to achieve groove angles of  $20^\circ$  or less, and in fact none of the techniques proved suitable for the present application. The Fourier synthesis methods [2,3,4] all require such high precision in the setting up of the interferometer that the task was beyond the scope of the present Contract. The Sheridan technique [5] was also ruled out because the maximum attainable groove angle (in a  $600\text{mm}^{-1}$  grating) is only about  $4^\circ$ . It was therefore decided that the possibility of making blazed "hard" gratings should be investigated.

#### 2.6.2 Hard Gratings

The interferometrically-generated photoresist mask used in hard grating manufacture may have either a blazed or a sinusoidal profile. Despite the fact that the Sheridan technique can only produce shallow groove angles, it is possible to exploit differential etch rates of photoresist and substrate material to achieve a steeper groove angle in the etched grating. For example, if an etch chemistry can be established in which silica is removed twice as fast as photoresist, then a groove angle of  $4^\circ$  in the resist grating can be increased to approximately  $8^\circ$  in the etched grating. Unfortunately, the largest "gain factors" achievable between photoresist and optical substrate materials such as glass and silica are around three, so that it is still not possible to achieve groove angles in the region of  $27^\circ$  as required (see Table 1).

Consequently, the technique which was eventually adopted was to start with a sinusoidal resist mask and use anisotropic (i.e. directional) etching to create a blazed profile in the hard grating. This work was carried out at the National Physical Laboratory, Teddington, UK under the supervision of Mrs S J Wilson. It is described in detail in her report, presented here as Appendix B. The main outcome of this work was that although it is possible to create an asymmetrical profile by this method, it is extremely difficult to obtain a sufficiently deep grating with a suitable groove angle. The target depth (see Table 1) for a silica grating is 760nm: the greatest depth achieved was 372nm. A reasonable degree of asymmetry was obtained: one grating (Sample 4 in Appendix B) gave 4.5 times as much light (at 458nm) in the -1 order compared with the +1. However, the zero-order transmission was still much larger than required. Inspection of the "Talystep" traces (a Talystep is a contacting surface-profile measuring instrument) showed that the "non-blazed" groove facets, whose groove angle should be  $(90-\theta)$  (i.e. over  $60^\circ$ ), had much smaller facet angles. In other words, instead of a sharp "saw-tooth" profile, the "teeth" were rounded and blunt. It was felt at this point that considerable further work would be required to obtain high-efficiency blazed gratings by this method.

### 3 GRATINGS WITH SYMMETRICAL GROOVE PROFILES

#### 3.1 Introduction

The difficulties encountered in attempting to fabricate blazed gratings with large groove angles were discussed with UCNW and USARDSG at a Contract progress meeting on 2 November 1989. At this time, UCNW made a small but significant change in the target specification by saying that their main concern was that the intensity of the zero-order transmitted beam should be reduced to about 4-5% of the incident intensity. The distribution of the remaining energy over the various diffracted orders ( $\pm 1$ ,  $\pm 2$  etc) was of only secondary importance. In all other respects, the target specification remained unchanged from that given in Section 2.2; the change simply removed the a priori requirement for a blazed groove profile.

#### 3.2 Sinusoidal Gratings

From an early stage of the Contract, it was clear that the gratings for use by UCNW were likely to be custom holographically-produced gratings, rather than commercially-produced ruled gratings. Consequently, once the use of gratings with symmetrical profiles became a possibility, the first profile to be considered was the sinusoidal one characteristic of holographic gratings.

Gale [6] presents a useful analysis whereby the zero-order efficiency of a transmission diffraction grating with a sinusoidal groove profile may be determined as a function of optical wavelength and/or groove amplitude. The relevant equation is

$$t(\lambda, a) = J_0^2(\pi a'(n_g - 1)/\lambda) = J_0^2(\pi a/\lambda) \quad (5)$$

where

$$t(\lambda, a) = \text{transmittance of grating (i.e. zero-order efficiency)}$$

$a$  = optical amplitude of grating (peak-to-peak)

$a'$  =  $a/(n-1)$  = physical amplitude of grating (peak-to-peak)

and  $J_0(x)$  = Bessel function of the first kind, order zero.

It is important to note that equation (5) is only strictly valid if  $d \gg \lambda$ , which is not the case for a  $600\text{mm}^{-1}$  grating used in the VNIR waveband. However, in the absence of a simple rigorous theory, equation (5) may be used to demonstrate the likely general trends in the variations of  $t(\lambda)$  with  $a$  and  $\lambda$ .

Gale's theory, if it can be shown to be at least approximately valid, is useful in two ways. First, it allows us to predict the peak-to-peak grating amplitude (i.e. groove depth)  $a'$  which will lead, for a given grating material, to  $t(\lambda)$  being minimised at a particular value of  $\lambda$ , e.g. 550nm. Secondly, the theory can also be used to infer  $a'$  from measurements of  $t(\lambda)$  at one or more values of  $\lambda$ . This is very useful as it represents at least a partial solution of a well-known "inverse problem" in the study of gratings, namely that of inferring information about groove amplitude and profile from measurements of the optical behaviour of a grating. Wilson and Botten [7] describe a similar technique for use with reflection holographic (i.e. sinusoidal) gratings.

Equation (5) predicts that  $t(\lambda, a)$  will be zero at  $\lambda = 550\text{nm}$  if  $a = 420\text{nm}$ , or that  $t$  will be zero at  $\lambda = 633\text{nm}$  if  $a = 483\text{nm}$ . The corresponding values of physical amplitude  $a'$  are presented in Table 2. In passing, it is interesting to compare the values of  $a'_{550}$  in Table 2 with those of groove depth in Table 1. Given the fact that in practice, the groove angles, and hence the groove depths, required to achieve peak blaze efficiency at 550nm are somewhat larger than the theoretical values shown in Table 1, there may well be some fundamental correspondence between blazed (triangular) gratings and sinusoidal gratings of equivalent depth.

Grating Material	$a'_{550}/\mu\text{m}$	$a'_{633}/\mu\text{m}$
Spectrosil-B	0.91	1.06
Schott BK7	0.81	0.94
AZ1350 photoresist	0.70	0.81

TABLE 2

Equation (5) may be used to plot  $t(\lambda, a)$  as a function of  $a$  for fixed  $\lambda$ , or as a function of  $\lambda$  for fixed  $a$ . Figure 3 shows  $t(0.55\mu\text{m}, a)$  versus  $a$  for  $0 < a < 0.75\mu\text{m}$ . The solid line is the theoretical curve given by equation (5), and the broken line is an estimate of the likely actual curve in the region of the minimum. This estimate is based upon the discrepancy between computed and measured transmittance suggested by Figure 2 of [6]. From the estimated "actual" curve it is possible to derive approximate values of  $a$  for actual gratings (see Section 3.4).

Figure 4 shows  $t(\lambda, 0.420\mu\text{m})$  versus  $\lambda$  for wavelengths between  $0.3\mu\text{m}$  and  $1.1\mu\text{m}$ . Once again, some discrepancy must be expected between this theoretical curve and actual measured values. Taken together, Figures 3 and 4 show that if there is a fixed waveband  $\lambda_{\min} < \lambda < \lambda_{\max}$  over which it is required to minimise  $t(\lambda, a)$ , then it is possible to choose a value of  $a$  for which the integrated transmitted flux  $P$  is minimised, where

$$P = \int_{\lambda_{\min}}^{\lambda_{\max}} P_0(\lambda) t(\lambda, a) d\lambda \quad (6)$$

where  $P_0(\lambda) =$  incident spectral flux (in  $\text{W } \mu\text{m}^{-1}$ ) at wavelength  $\lambda$

However, if the waveband of interest is approximately  $0.4\mu\text{m}$  to  $1.1\mu\text{m}$ , then the above approach is likely to lead to a graph of  $t(\lambda)$  vs  $\lambda$  which has a local maximum (of about 15%) somewhere near the middle of the visible spectrum. If this is unacceptable, then either some compromise must be sought in which the need to minimise  $t(\lambda)$  is accepted to be more pressing in some parts of the waveband of interest than in others, or the effects of gratings with non-sinusoidal groove profiles must be investigated.

Alternatively, the actual requirement may be to minimise  $t(\lambda, a)$  at a number of specific laser wavelengths. In this case, we write

$$P = \sum_n P_n(\lambda_n) t(\lambda_n, a) \quad (7)$$

where  $\lambda_1, \lambda_2 \dots \lambda_n$  are the wavelengths of interest and  $P_n(\lambda_n)$  is the incident flux at  $\lambda_n$ . This may ease the problem a little, but difficulties will still remain if one or more of the laser wavelengths occurs at or near a local maximum. It is therefore useful to consider how graphs like Figures 3 and 4 will change if the groove profile is symmetrical but non-sinusoidal.

### 3.3 Non-Sinusoidal Gratings

Gale [8] presents a brief discussion of the zero-order transmission characteristics of gratings with non-sinusoidal profiles. Figure 5 shows graphs of  $t$  versus  $a/\lambda$  for six different profiles. In order that the transmission should remain low over the waveband  $0.3\mu\text{m} < \lambda < 1.1\mu\text{m}$ , it is necessary to find a profile and a region of the corresponding graph such that  $t(a/\lambda)$  is small for  $x < a/\lambda < 3.66x$ . This is quite a large range. Clearly, profiles a), b) and c) (sinusoidal, lens and triangle) are likely to be more suitable than d), e) or f) (square, rectangle or triple step).

For a grating with a surface relief function  $s(x)$ , it can be shown that for  $d \gg \lambda$ , the zero-order transmission  $t(\lambda)$  is given by

$$t(\lambda) = \left\{ (1/d) \int_0^d \exp(2\pi i s(x)(n_g - 1) \lambda) dx \right\}^2 \quad (8)$$

For a symmetrical triangular grating of peak-to-peak amplitude  $a'$ , we have

$$s(x) = \begin{cases} -2a'x/d + a'/2, & 0 \leq x \leq d/2 \\ 2a'x/d - 3a'/2, & d/2 \leq x \leq d \end{cases} \quad (9)$$

Substituting equation (9) in equation (8) and simplifying, we obtain

$$t(\lambda, a) = (\sin^2 \pi a'(n_g - 1)/\lambda) / ((\pi a'(n_g - 1)/\lambda)^2)$$

i.e.  $t(\lambda, a) = \sin^2 (\pi a/\lambda) / (\pi a/\lambda)^2 \quad (10)$

It is interesting to compare equations (5) and (10). Figure 6 shows the two functions in the region  $2 \leq \pi a/\lambda \leq 12$ .  $t(\lambda, a)$  falls to zero more rapidly for a sinusoidal grating than for a triangular one: the first zeros occur at  $\pi a/\lambda = 2.4$  and  $\pi$  respectively. So, given the fact that gratings become harder to fabricate (by whatever means) as  $a$  increases, if the requirement were simply to achieve  $t(\lambda, a) = 0$  for a single wavelength, then a shallower grating will suffice if the profile is sinusoidal. However, the actual requirement is for  $t(\lambda, a)$  to remain small over an extended waveband, and Figure 6 makes it clear that, as long as a sufficiently deep grating can be fabricated, this requirement will be more closely met by a grating with a triangular profile.

### 3.4 Fabrication of Symmetrical Gratings

Once the requirement for a blazed groove profile was removed, the main objective of the fabrication work became to achieve a sufficiently large

groove depth in a symmetrical grating. Such a grating could now be either a deep sinusoidal photoresist grating, or a symmetrical etched grating. Given that during the dry-etching process it is usually more difficult to increase groove depth than to decrease it, the best starting point for the etched grating was also a deep sinusoidal resist grating. In this case however, there is an additional requirement to minimise the "DC level", i.e. the thickness of resist below the sinusoidal modulation (see Figure 7).

Figure 3 shows that the target depth  $a'$  for a sinusoidal grating in photoresist to exhibit minimum transmission at 550nm is about 700nm. In a photoresist grating, the depth is determined by a number of factors including the type of photoresist used, the concentration of the solution, the spin speed during spin coating, the fringe contrast in the interferometer, the exposure time, the developer type and concentration, and the development time. In an extension of their programme beyond the work described in Appendix B, NPL made a number of sinusoidal resist gratings, varying several of the parameters listed above in an attempt to achieve a suitable groove depth. After testing at CCL, two of the most successful of these were chosen for delivery to UCNW. The serial numbers are C3086/01 and C3086/03; detailed specifications of numbered gratings are presented in Appendix C. The groove amplitudes were inferred from measurements of the zero-order transmission, using graphs similar to Figure 3. The resulting estimated values of  $a'$  were 755nm and 650nm for C3086/01 and C3086/03 respectively.

NPL next proceeded to attempt to make a hard grating with a similar groove amplitude. Photoresist grating no C3086/23 was chosen as a suitable mask, since it exhibited low zero-order transmission in the mid-visible, viz 5% at 543nm. Figure 3 suggests that this would imply a groove amplitude of over 800nm. However, after etching, the zero-order transmission had increased to 33% at 543nm, and so clearly the profile had not been faithfully reproduced in the substrate. Talystep measurements suggested that the amplitude  $a'$  was still over 520nm, but for depths over about 400nm the Talystep is no longer a very precise indicator of either groove depth or profile for gratings as fine as  $600\text{nm}^{-1}$ . So, it is possible

that the groove profile of C3086/23 after etching was tending towards the undesirable "square-edged" shapes of Figure 5 d) e) and f).

NPL made one further attempt to achieve low zero-order transmission in the mid-visible (i.e. around  $\lambda = 550\text{nm}$ ) with an etched grating. Grating no C3086/14 had a transmission of 7% at 543nm before etching. In view of the difficulties encountered with C3086/23 and other attempts at producing symmetrical etched gratings, it was decided to check the performance of the grating at intermediate stages of the etching process, i.e. before all the photoresist was removed. At one such stage, it was found that the transmission at 543nm had actually decreased very slightly to 6%. Further tests showed transmissions at 594nm, 633nm and 875nm of 3%, 5% and 6% respectively. Since this excellent broad-band zero-order attenuation had not been observed with any other grating (hard or soft), it was decided not to proceed with any further etching but to deliver the grating to UCNW. Consideration of Figure 5 suggests that the profile is likely to be some fortunate combination of triangular and sinusoidal<sup>1</sup>, with a minimum depth of over  $1\mu\text{m}$ .

In parallel with the programme of symmetrical grating fabrication at NPL, a short piece of work was also commissioned from Leybold AG of West Germany. The aim was to investigate the feasibility of using a parallel-plate reactive ion etching system to manufacture deep symmetrical hard gratings. The parallel plate system differs from the Kauffman ion beam system used by NPL in that it in general can only be used for isotropic, i.e. non-directional, etching. It is therefore not suitable for the fabrication of blazed gratings, and was not considered as a possible technique during the earlier stages of the project. Photoresist masks were prepared by NPL, with the aim of producing gratings similar to C3086/23 and C3986/14. These were then sent to Leybold AG, with a description of the "ideal" etched grating. Two etched gratings (3086/05 and /10) were later received from Leybold, tested at CCL and supplied to UCNW.

C3086/05 showed zero-order transmission values of 45.6% at 633nm and 64.1% at 870nm. These figures both suggest that the grating is approximately sinusoidal, with a groove amplitude of about  $0.55\mu\text{m}$ . The

other grating (C3086/10) showed transmissions of 15.0% at 458nm, 2.0% at 633nm, and 20.8% at 875nm. The particular interest in this grating was that some scanning electron micrographs were taken which showed the groove profile very clearly (see Figure 8). The upper part of the profile (the groove "crests") appears approximately sinusoidal, while the lower part (the groove "troughs") is more flattened and shows a tendency to "squareness". Furthermore, the groove amplitude may be determined from the SEM photographs to be 870nm ( $\pm 10\%$ ). We may therefore re-plot graphs such as a) and d) of Figure 5 to show  $t(\lambda, a' = 870\text{nm})$  for wavelengths between 450nm and 900nm, and then compare the graphs with the actual measured values at the three wavelengths mentioned above. The graphs are shown in Figure 9, and it is pleasing to note that by considering grating C3086/10 as basically sinusoidal but with a small square-wave "perturbation", we can see that (i) at 633nm,  $t(\lambda)$  will be low because the sinusoidal profile graph is close to its first minimum, and the square-wave graph is also low: (ii) at 458nm,  $t(\lambda)$  will be considerably greater than the "sinusoidal" value because the square-wave perturbation is very large: and (iii) at 875nm, the effect of the square-wave perturbation will be slightly to reduce the  $t(\lambda)$  value predicted by the sinusoidal graph. Thus the observed values of  $t(\lambda)$  match the predicted ones quite well, and provide reassuring evidence for the validity of Gale's theory as at least a qualitative indicator of the ways in which groove amplitude and profile affect zero-order transmission.

It is pleasing to note that gratings C3086/10 and C3086/14 meet the revised target specification (see Sections 2.2 and 3.1) in most respects. C3086/10 offers excellent attenuation at 633nm, but is rather small (although large enough for most types of laser testing). C3086/14 offers good broad-band attenuation and is larger, but is not fully "hardened". (It is not clear how much photoresist remains on C3086/14, or what the effect on performance would be if it were removed). It was unfortunately not possible within the scope of the present Contract to commission a large-area version of C3086/10 from Leybold. However, a large-area photoresist mask similar to that used for C3086/10 was supplied to Electrotech Ltd (Bristol UK) for reactive ion etching.

The resulting hard grating (C3086/21) is non-uniform, in that the zero-order transmission is considerably higher in a central circular region (radius  $< 13\text{mm}$ ) than in the peripheral annular region ( $13\text{mm} < r < 25\text{mm}$ ): the substrate diameter is  $50\text{mm}$ . Because of the non-uniformity, the grating has not been tested in detail, but an outline specification is presented in Appendix C. The peripheral region appears dark blue in transmitted light, which suggests that the groove depth here is only slightly less than that in C3086/10. The non-uniformity could be caused by a corresponding non-uniformity in the photoresist mask (for example, a radial variation in the photoresist DC level), but the strangely sudden transition between the central and peripheral behaviour suggests that some artefact of the plasma processing may be the cause. The substrate is considerably thicker ( $5\text{mm}$ ) than is the case with C3086/10, say, and it is possible that the central region may have become rather hot during the etching process. As is suggested in Section 4 below, further investigation of C3086/21 could prove useful.

#### 4 CONCLUSIONS AND RECOMMENDATIONS

##### 4.1 Conclusions

This Contract has shown that, in order to achieve a good, broad-band zero-order attenuation using a  $600\text{mm}^{-1}$  transmission diffraction grating, it is necessary to control both the amplitude and the profile of the grating grooves. It is not essential that the grating has a blazed profile, which is fortunate since the early stages of the Contract showed that it would be extremely difficult to achieve a sufficiently large blaze angle while retaining a "sharp" saw-tooth profile.

Turning to gratings with symmetrical profiles, it is also clear that it is quite difficult to achieve a sufficiently large groove amplitude in an interferometrically-produced photoresist grating. Photoresist (and epoxy) gratings may of course eventually have to be ruled out on the grounds of low laser damage threshold, but even in the short term (eg during the course of the present Contract), larger amplitudes, and hence greater zero-order attenuations, are generally easier to achieve using dry-etching techniques. There is some evidence that better results can be achieved using a parallel-plate reactive ion etching system, rather than a collimated ion beam system such as was used by NPL. The former system does not however offer much scope for generating asymmetrical groove profiles, should this ever be a requirement.

It has been shown that dry-etching techniques can be used to achieve the required groove amplitudes (values in the region of  $1\mu\text{m}$  for  $600\text{mm}^{-1}$  gratings). It is also clear that the next step is to refine the etching techniques such that the groove profile may also be well-controlled. For example, for good broad-band zero-order attenuation a (symmetrical) triangular profile would appear from this work to be the aim.

A more general conclusion which may be drawn is that successful fabrication of broad-band attenuating gratings requires all stages of the manufacturing process to be carefully controlled. The respective etching behaviour of both the photoresist and the substrate material must be taken

into account in the design of the optimum photoresist mask. Ideally, the mask itself should then be tested for conformity with specification prior to dry etching. The etching process must also be well-controlled, and if possible some form of end-point detection should be devised.

In summary, we may state that once the processes identified during the present Contract have been optimised as described above, it will be possible to fabricate hard transmission gratings (on flat substrates) with the groove amplitude and profile controlled to achieve a broad-band VNIR zero-order attenuation of around 95%, ie an optical density of  $\sim 1.3$ . Some suggestions for future work are presented below.

#### 4.2 Recommendations

##### 4.2.1 Process Optimisation

The present Contract has clearly demonstrated the feasibility of making suitable gratings by the reactive ion etching of photoresist masters. The most pressing need now is to optimise process parameters so that gratings with controlled groove amplitude and profile may be made in a reliable and repeatable fashion. This work will include a theoretical and empirical investigation of the photoresist process, geared specifically to provide optimum "masters" for the etching process. Consideration will be given to mask fabrication using conventional photolithography as well as the interferometric approach used in the present Contract. Optimisation of the reactive ion etching process will be carried out in parallel with the photoresist work. This will involve for example, the determination of precise etch rates, for both photoresist and substrate material, using a variety of etch chemistries: the establishment of techniques for accurate control of groove amplitude: and the investigation of ways of achieving the desired groove profile.

##### 4.2.2 Device Manufacture and Test

Once the process optimisation described above is complete, it will be possible to manufacture a second batch of etched gratings whose

performance should closely match UCNW/USARDSG's requirements. For example, the gratings may be designed to achieve good broad-band rejection right across the VNIR band, or may be fabricated on "black glass" substrates (which absorb IR energy) so that diffractive rejection is required in the visible band only. Alternatively, attention may focus on achieving good rejection at specific laser lines only. In any case, it will be important to carry out detailed tests on all gratings produced, to establish the fidelity with which the target performance has been achieved. These tests will include detailed spectral transmission measurements, with both s- and p-polarised light and at normal and off-axis incidence. It would also be sensible to establish LIDT (laser-induced damage threshold) values at (for example) 532nm, 694nm and possibly 1064nm.

#### 4.2.3 Optical Switching

The present contract has shown that a single, deep-grooved transmission diffraction grating can provide a broad-band zero-order attenuation of around 95%, i.e. optical density 1.3. Two "crossed" gratings can probably increase the density to well over 2. However, when we consider the use of these gratings as protection devices against high-energy pulsed lasers in either visual or electro-optical sensor systems, a compromise must clearly be sought between the level of protection provided and the optical performance (e.g. in terms of image luminance or radiance) of the sensor. Ideally, what is required is a fast-acting "switch" which "turns on" the protection device only when a threat is encountered. The main requirements for such a device are (a) low insertion loss, i.e. low optical attenuation in typical ambient operating conditions, and (b) rapid switching to a suitably high optical attenuation at a well-defined activation energy, i.e. in response to a potentially damaging pulse. Other desirable features would include broad-band response, high LIDT and of course reasonable production cost.

Over the last few months, CCL has derived a conceptual design for a device which might go some way towards meeting these requirements. Our proposed device is based upon a crossed high-efficiency surface-relief diffraction grating, index-matched to a polymer layer such that the grating remains inoperative under normal conditions of illumination.

Cambridge Consultants Ltd  
C3086-FR-001a

Suspended in the polymer layer, however, are absorbing particles which, above a certain energy threshold, will promote the formation of microbubbles which will locally remove the index-matching of the grating. A high proportion of the incident pulse energy can thereby be diffracted out of the field of view of the viewing system. Our preliminary analysis suggests that such a device could have an activation energy in the range 1-10 $\mu$ J, an insertion loss of 40-60% and an optical density when activated of 2 to 2.5 over the VNIR band.

If it is agreed that these ideas are worthy of further consideration, then the next step would be to carry out a detailed theoretical and experimental programme to establish the feasibility of the proposed device. This programme could be carried out in parallel with the further development of gratings described in Sections 4.2.1 and 4.2.2 above, and indeed would almost certainly benefit from the process optimisation work described in Section 4.2.1.

REFERENCES:

- 1 Hutley, M.C.: "Diffraction Gratings", Academic Press (1982).
- 2 Rudolph, D. and Schmahl, G.: UK Patent no. 1261213 (1968).
- 3 Bryngdahl, O.: J. Opt. Soc. Am. 60, 140 (1970).
- 4 McPhedran, R.L., Wilson I.J. and Waterworth M.D.: Opt. Laser Technol. 5, 166 (1973).
- 5 Sheridan, N.K.: Appl. Phys. Lett. 12, 316 (1968).
- 6 Gale, M.T.: Opt. Commun. 18, 292 (1976).
- 7 Wilson, I.J. and Botten, L.C.: Appl. Opt. 16, 2086 (1977).
- 8 Gale, M.T. and Knop, K.: "Surface-relief images for color reproduction", Focal Press (1980).

FIGURES

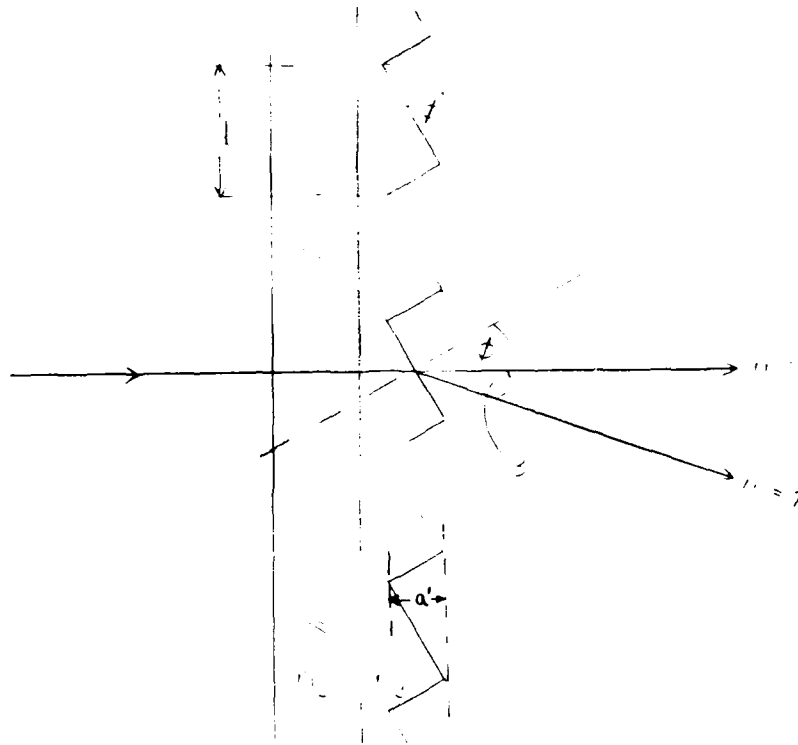


FIGURE 1: Blazed Transmission Diffraction Grating

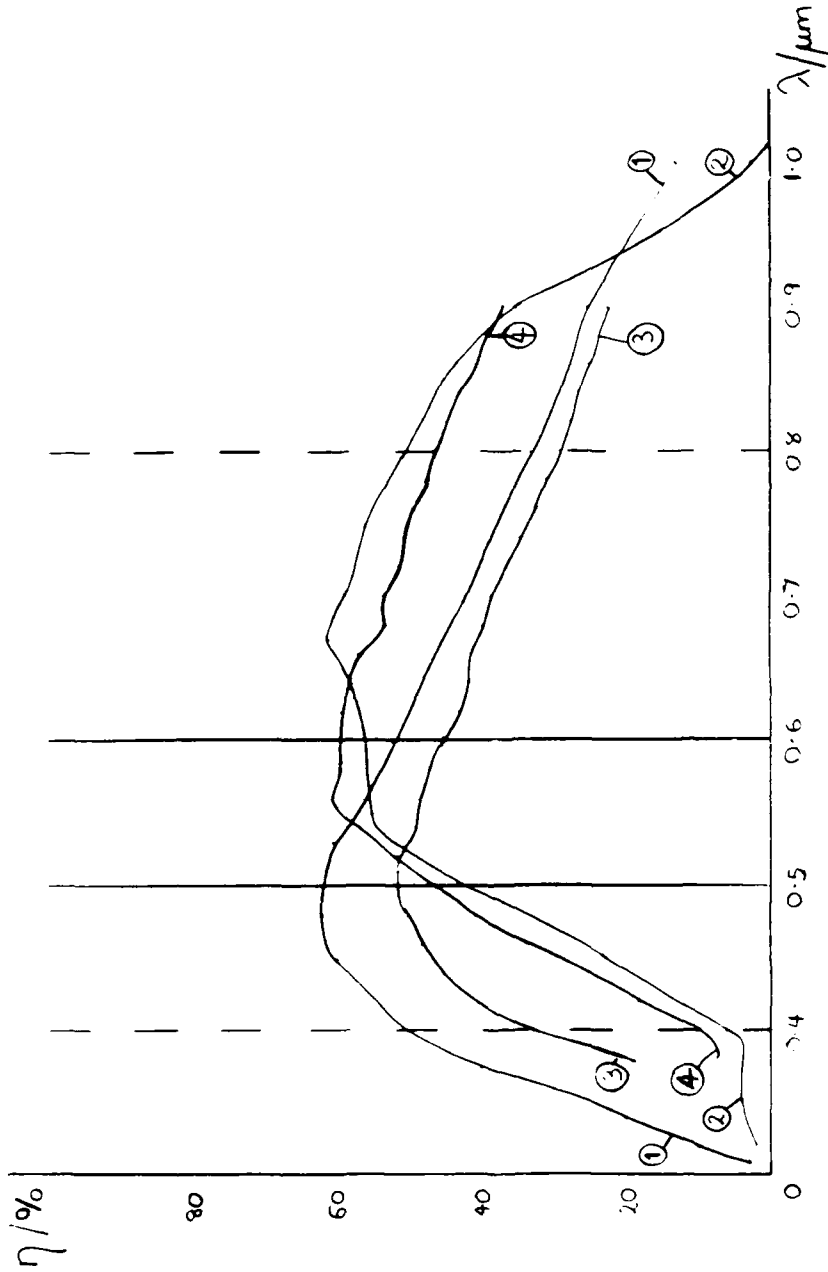


FIGURE 2: Efficiencies of Commercial Replica Gratings

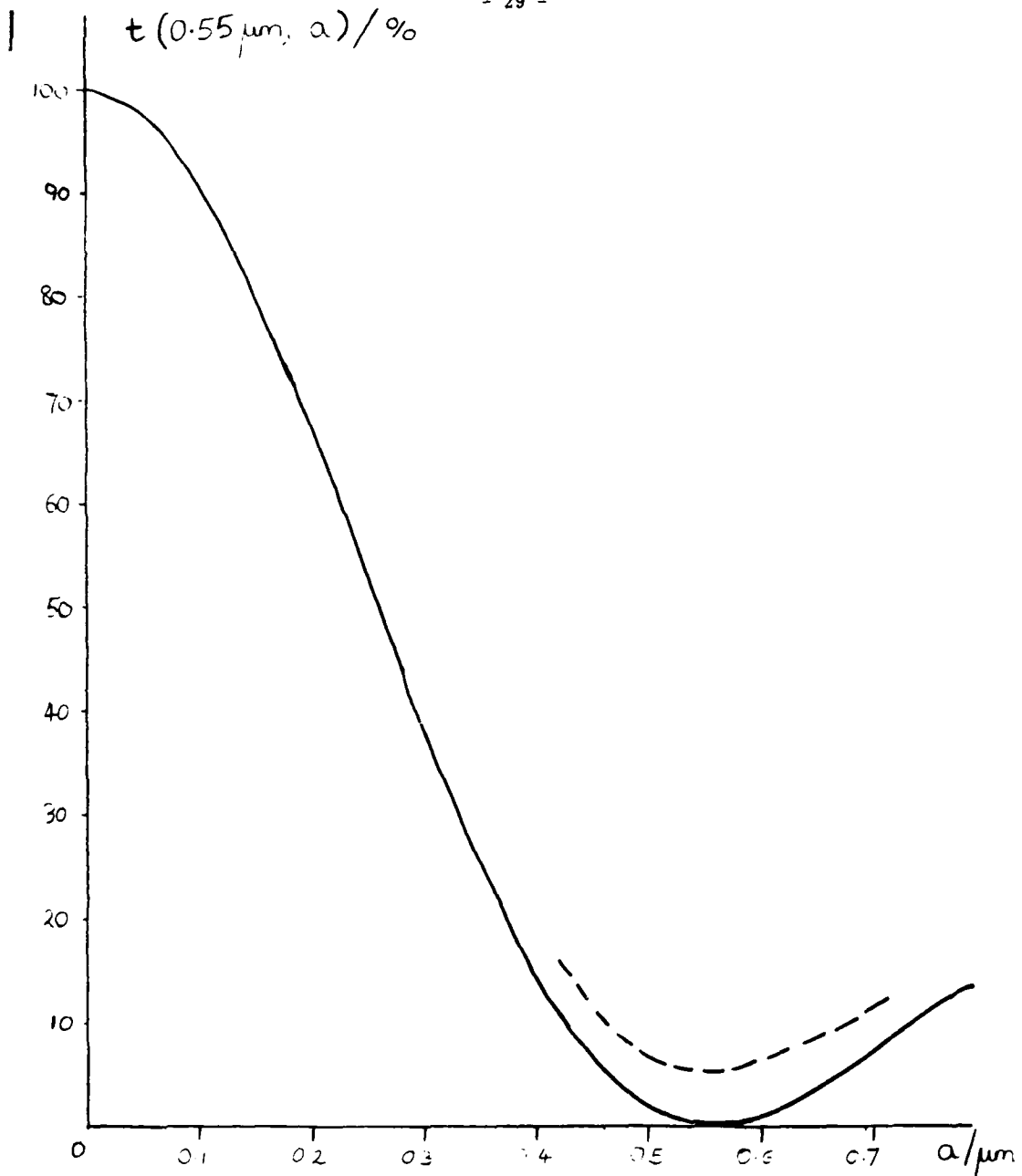


FIGURE 3:  $t(0.55 \mu\text{m}, a)$  vs  $a$

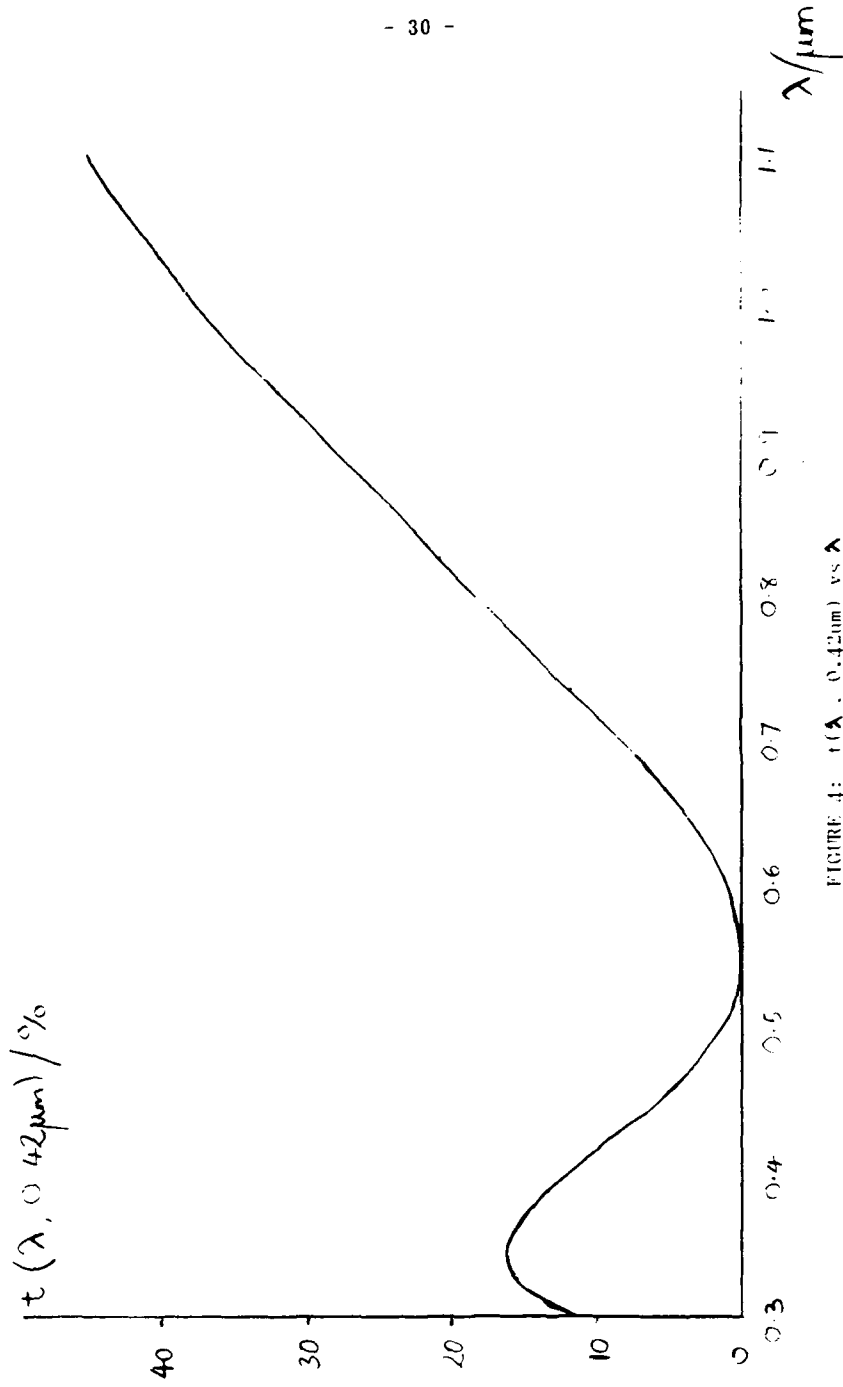


FIGURE 4:  $t(\lambda, 0.42\mu\text{m})$  vs  $\lambda$

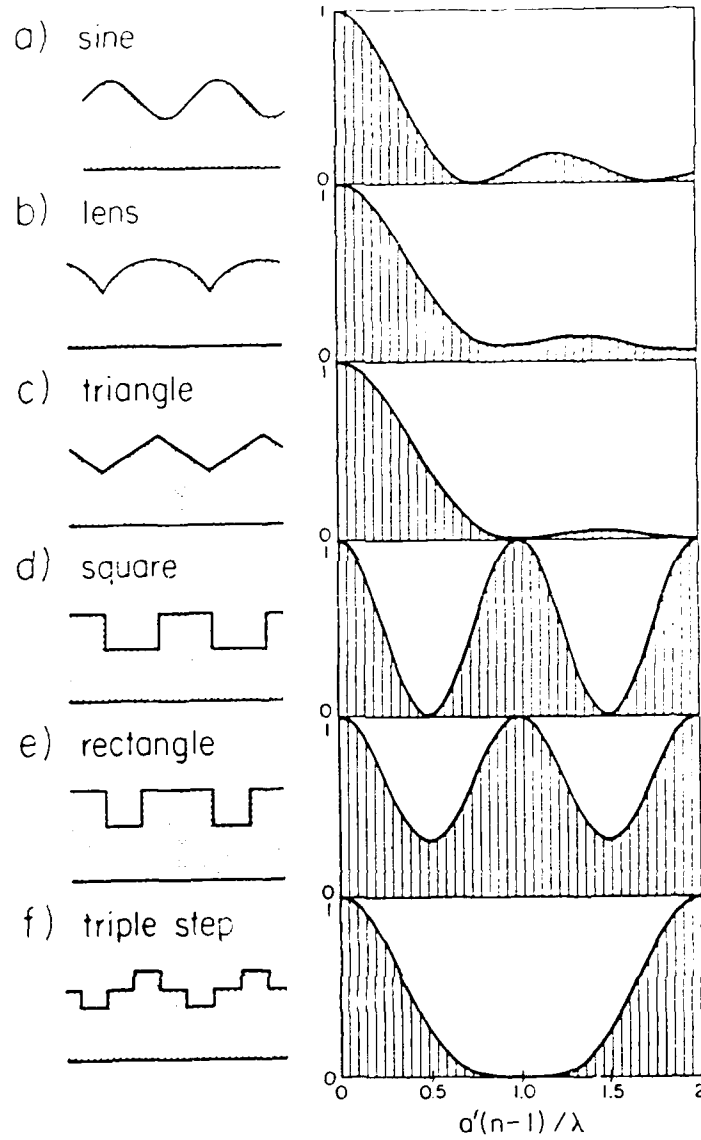


FIGURE 5: Zero-order transmission characteristics of various phase gratings (from reference 8).

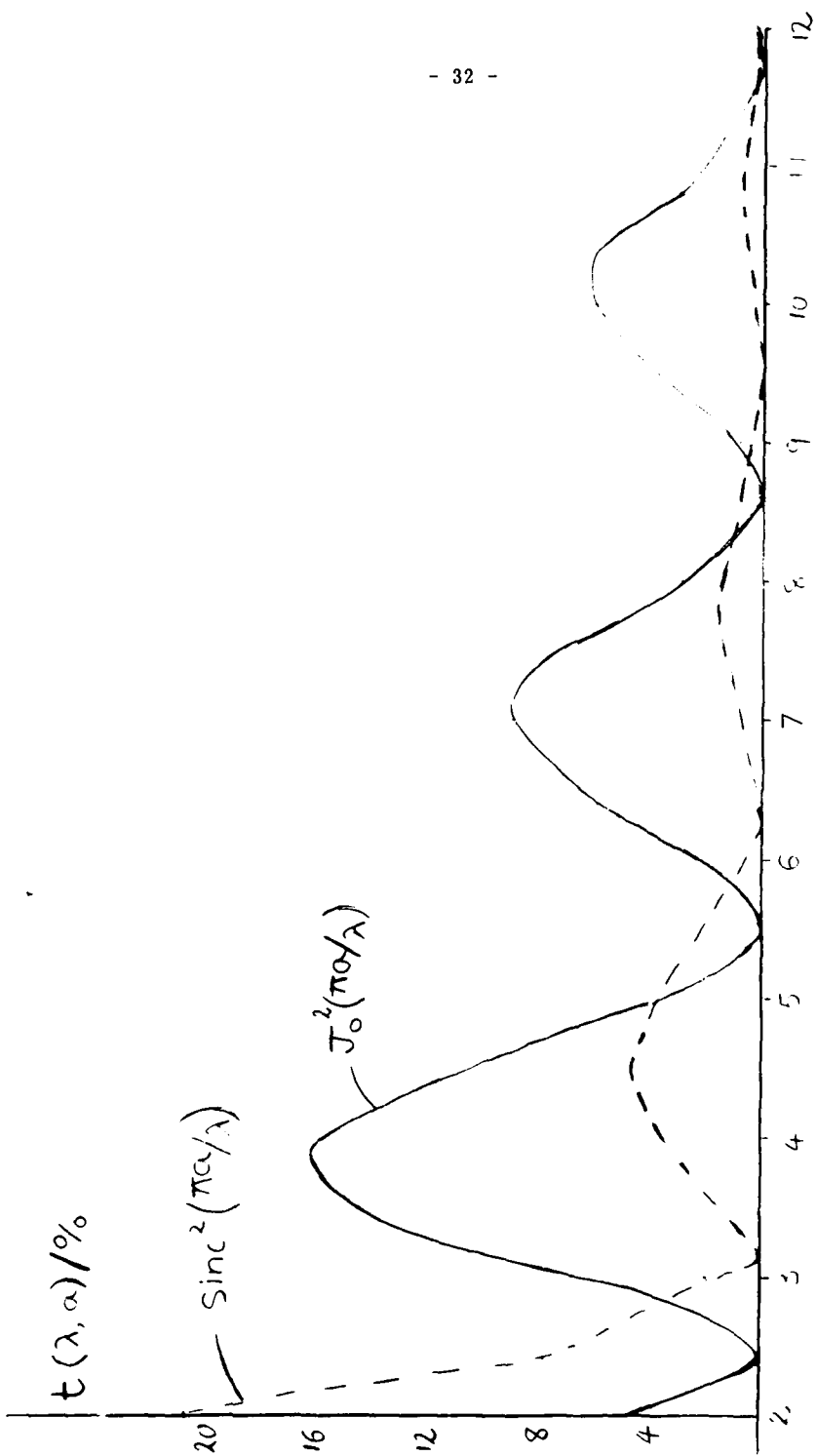


FIGURE 6: Zero-order transmission of sinusoidal grating (solid line) and triangular grating (broken line)  $\pi_0 \lambda$

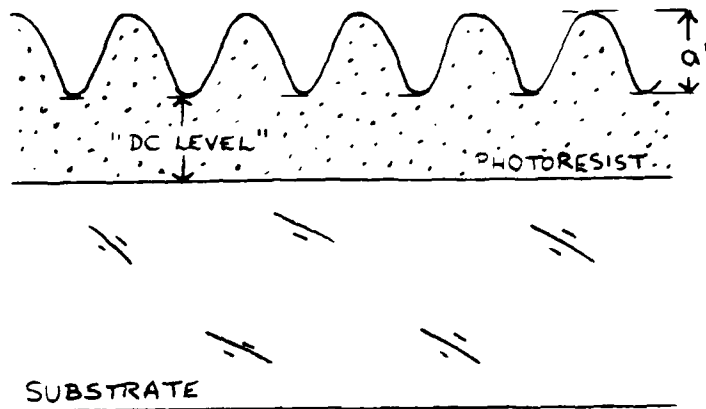


FIGURE 7: "DC level" in photoresist grating



FIGURE 8: SEM photographs of grating no C3086/10

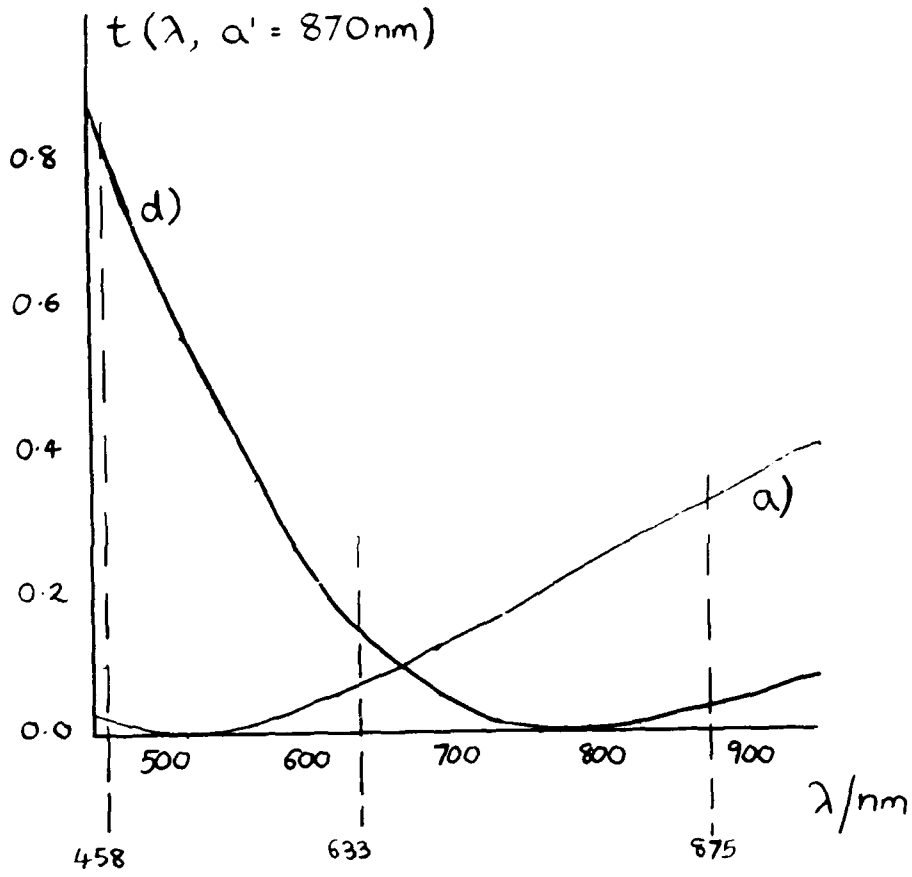


FIGURE 9:  $t(\lambda, a' = 870\text{nm})$  vs  $\lambda$ : a) sinusoidal profile, d) square profile

APPENDIX A: Commercial Blazed Transmission Gratings

Prior to this Contract being placed, UCNW had been unable to identify any suitable, commercially-available replica gratings. During Phase I of the Contract, CCL identified a number of such gratings which could be of some limited use to UCNW. These included the two Milton Roy gratings mentioned in Section 2.5, and two others manufactured by Hyperfine Inc. of Boulder CO, USA. Traces (3) and (4) on Figure 2 refer to these Hyperfine replica gratings. UCNW indicated that grating (4) would come closest to meeting their requirements, and so three of these gratings were obtained and supplied to UCNW. The specification is as follows:

Grating type : blazed transmission grating

Frequency :  $600\text{mm}^{-1}$

Blaze angle :  $31.6^\circ$

Substrate material : Schott glass type BK7

Substrate index : 1.52 at 633nm

Substrate diameter : 50mm

Substrate thickness : 10mm

Grating material : Shell 834 epoxy resin

Grating index : 1.59 at 633nm

Coating : single-layer  $\text{MgF}_2$  antireflection coating (optimised for 700nm) on non-grating surface of substrate.

Tests carried out by CCL prior to the despatch of these gratings to UCNW indicated that the first-order efficiency is about 58%, with some 5 to 10% of the incident intensity remaining in the zero order.

Once again, it is noted that although these gratings were labelled "blazed at 700nm", presumably because equation (4) gives  $\lambda_b = 700\text{nm}$  if  $\theta = 31.6^\circ$ , the measured blaze wavelength is in fact shifted down to about 560nm. This result is in accordance with those for gratings (1) and (2) of Figure 2, and suggests a rough rule-of-thumb for  $600\text{mm}^{-1}$  blazed gratings that the actual blaze wavelength is about 80% of the theoretical one.

APPENDIX B: NPL Report

C3086-FR-001a

Cambridge Consultants Ltd

An investigation into the feasibility of ion etching  
600 g/mm transmission gratings for the mid-visible

by

MRS S J WILSON, NPL

Work carried out for Cambridge Consultants Ltd

Cambridge Consultants Ltd

TO INVESTIGATE THE FEASIBILITY OF ION ETCHING 600 g/mm  
TRANSMISSION GRATINGS BLAZED FOR THE MID-VISIBLE

The work was preceded by a round table discussion at Cambridge Consultants Ltd.

Present: Tom Empson )  
Tomas Gesang ) CCL  
Roger Miller )  
Sylvia Wilson NPL

AIM

A 600 g/mm transmission grating with a blaze angle of  $26^\circ$  ion etched into silica or BK7.

ETCHING EQUIPMENT

NPL has an Oxford Applied Research ion beam etched fitter with a Kauffman gun which produces a 150 mm dia collimated beam of argon ions. The substrate holder can be tilted with respect to the ion beam. Reactive gases such as freon, oxygen etc can be introduced into the vacuum chamber in order to change the relative etch rates of mask and substrate materials.

ETCH MASK

Two possibilities were considered.

a) Blazed photo resist etch mask

Good quality blazed photo resist gratings can be made by the NPL/Sheridon technique but only blazed for reflection in the UV. For a 600 g/mm grating  $\theta_B = 3^\circ 26'$ . This profile could be transferred to the substrate by etching normal to the surface at the same time increasing the blaze angle ie the depth of the grating, by a factor of 7 approx.

This approach has been used successfully at NPL to produce X-ray  
Cambridge Consultants Ltd

gratings<sup>1</sup>. Etch conditions had been chosen to produce a reduction in depth of the grating. However as far as our increase in depth is concerned, at the present time, the maximum etch rate ratio that had been achieved between photo resist and silica was between 2 and 3. This is not sufficient.

b) Sinusoidal photo resist etch mask

The grating could be transferred to the substrate, the blaze being produced by etching at an angle to the grooves. Matsui *et al*<sup>2</sup> and Ayogai and Namba<sup>3</sup> had reported success using the technique to produce blaze angles up to 27°. They had used reactive ion beam etching to obtain an etch rate ratio of 2.8 which corresponds with that which NPL can achieve. Efficiencies of the etched gratings were not reported in the paper.

WORK PROGRAMME

After discussion it was decided to use a sinusoidal grating as an etch mask and the conditions laid out in the Matsui paper be used as a starting point. CCL would provide up to 10 samples of 600 g/mm gratings on silica to be etched by NPL.

EXPERIMENTAL WORK

In the event CCL were unable to provide suitable samples within the necessary time scale and it was considered to be more efficient if the whole process was carried out in the same place.

PREPARATION OF SAMPLES

Substrates:	30 mm dia Spectrosil B (fused silica)
Photo-resist:	Shipley Microposit 1400-17
Coating:	Spin coating with Headway spinner
Pre-bake:	60 °C for 30 mins
Exposure source:	Argon ion laser, 600 mW at 457.9 nm
Development:	Microposit developer, 5 seconds
Part-bake:	100 °C for 16 hours

Resist coatings were made of several thicknesses. In each case about 4 gratings were made with differing exposures and the deepest grating was

selected for etching. The maximum depth of grating that could be made was less than the original resist thickness due to interference effects at the resist/silica interface.

#### ETCHING OF GRATINGS

$C_2F_6$  (Halocarbon R116) was used as the reactive gas. From previous experiments this gave a typical etch rate ratio of 2.5:1 for silica/1400-17 photo resist. This corresponded with that used by Matsui et al.

The grating grooves were set perpendicular to the angle of tilt of the substrate platen so that only one side of the grooves were bombarded with ions. The platen or substrate holder was cooled with chilled water but because the silica is a poor conductor of heat and the photo resist had to be kept below  $100^\circ C$  to prevent damage to the grating, etching took place in bursts of  $1\frac{1}{2}$  to 2 minutes with 5 minutes intervals during which time the ion beam was shuttered.

#### ETCHING CONDITIONS

Platen angle  $64^\circ$  (see graph 1)

Base press in vacuum chamber  $5 \times 10^{-6}$  mb

Chamber press with argon flowing through gun  $1.3 \times 10^{-4}$  mb

Chamber press with argon through gun and  $C_2F_6$  through gas dispense ring  $4.0 \times 10^{-4}$  mb

Ion gun parameters	Beam voltage	400V
	Beam current	100 mA
	Accelerator voltage	300V

#### SAMPLE 1

Resist: 1400-17 diluted 1:2 Microposit thinners

Spin speed: 1700 rpm

Nominal thickness:  $1220 \text{ \AA}$

Depth of grating:  $510 \text{ \AA}$

Etch time: 23 mins

Depth of grating after etching  $1000 \text{ \AA}$

#### RESULTS AND COMMENT

Talystep traces show the depth of grating had increased by a factor of 2. The etched profile was not good and showed little asymmetry.

Since the ideal depth of the grating was  $7000\text{\AA}$  and in practice for a reasonably efficient grating would be around  $5000\text{\AA}$  it is difficult to see how this depth can be achieved starting with a photo resist grating of only  $500\text{\AA}$  depth. Even if the depth were that of the original photo resist coating ie  $1300\text{\AA}$  quoted by Matsui this would seem improbable. However it was worth checking.

#### SAMPLE 2

Resist: 1400-17 diluted 4:3  
Spin speed: 1700 rpm  
Nominal thickness:  $3700\text{\AA}$   
Depth of grating before etching  $1080\text{\AA}$   
Depth of grating after etching  $3000\text{\AA}$   
Total etch time: 23 mins

After 20 mins etching the sample was removed from the vacuum system and Talystep profiles taken. The resist was not fully etched through at this stage. There was a pronounced asymmetry and the grating depth had increased to  $3000\text{\AA}$ .

The grating was masked, put back in the vacuum system and etched for a further 3 minutes to remove the remaining traces of photo resist.

#### RESULTS AND COMMENT

From the Talystep profiles the projected depth of the grating was  $5000\text{\AA}$  with a blaze angle of  $20^\circ$ . Although the grating was unsymmetrical the depth of the modulation was not sufficient to produce a very efficient grating.

Two possibilities were considered.

- (1) To make a deeper grating in photo-resist
- (2) To alter the platen angle to get the correct blaze angle.

I decided to go for a deeper grating in resist to try to improve the  
Cambridge Consultants Ltd

overall depth and therefore the efficiency.

SAMPLE 3

Resist: Microposit 1400-17 neat  
Spin speed: 7250 rpm  
Nominal thickness  
Total depth of resist after processing 6790Å  
Depth of grating 4200Å  
Depth of resist below grating 2590Å  
Total etch time 90 mins - resist still on surface

The depth of resist below the grating was considerable. It would be possible to take the grating down to the substrate using oxygen etching but this required further and possibly lengthy etch trials. I decided to try etching the specimen to see what profile could be achieved.

Talystep traces were taken after 50 mins etch. Slight asymmetry of resist grating.

At 70 mins asymmetry was pronounced. Although some resist remained on surface efficiency measurements were made.

$\lambda = 543 \text{ nm}$

GRATING ORDER	+1	0	-1
S POL	10	20	54%
P POL	10		50

When the resist was later removed from this part of the etched area a Talystep trace showed the grating was partly etched into the silica at this stage.

At 90 mins the resist was still not etched through but by now was badly undercut as indicated by the Talystep traces which gave approximately the same asymmetric profile in each direction as if the resist was being bent over by the stylus. Removal of the resist showed the silica grating to have far from the ideal profile.

COMMENT

The results were encouraging although the blazed grating was only produced at an interim stage. Another grating was made in thinner resist

Cambridge Consultants Ltd

to try to reduce the amount of "DC" level below the grating.

SAMPLE 4

Resist: Micropoint 1400-17  
Spin speed: 3000 rpm  
Nominal thickness 5500Å  
Total depth of resist after development 4260 Å  
Depth of grating 3720 Å  
Depth of resist below grating 540 Å  
Total etch time 60 mins

The grating was masked at intervals, Talystep traces being taken at each stage. Finally the resist was removed from the grating by wiping with acetone so that traces could be made on the silica.

Areas were masked to give four strips of grating etched for 35, 40, 50 and 55 mins. Talystep traces were taken at each stage. The substrate was then remasked at right angles to the strips and then etched for a further 5½ mins. The beam voltage was accidentally 600 instead 400. further Talystep traces were taken and finally the resist was removed from the grating by wiping with acetone so that measurements could be made on the 8 areas of grating.

RESULTS AND COMMENT

Efficiency measurement in transmission

Grating: 55 min  $V_B$  400 + 5½ min  $V_B$  600

Grating Order

$\lambda$ (nm)	POL	Grating Order		
		+1	0	-1
458	S	10	25	48
	P	11	31	41
514	S	11	42	31
	P	10	35	33

From the Talystep traces the projected depth was  $\sim 8000\text{\AA}$  with a blaze angle of  $26^\circ$ . The traces do not show a very good blaze. Efficiency measurements showed a 4.5:1 ratio between -1 and +1 at 458 nm.

Recalculation of the blaze wavelength for  $26^\circ$  gave  $\lambda_B = 388\text{ nm}$ . Unfortunately it was not possible to measure the efficiency at this wavelength.

#### CONCLUSION

Gratings can be blazed by this technique but a considerable amount of further work is needed to obtain high efficiencies. This includes an investigation into the variation of etch rate with angle of incidence of the ion beam in the presence of a reactive gas and possibly some computer modelling of the evolution of the groove profile. The fact that it was not possible to reproduce the results obtained by Matsui, Namba et al is supported by a paper by Johnson<sup>4</sup> although this refers to ion beam etching in argon. It should be pointed out that a blaze angle of  $33^\circ$  is needed for the mid-visible which would probably be more difficult to achieve than  $26^\circ$ .

#### REFERENCES

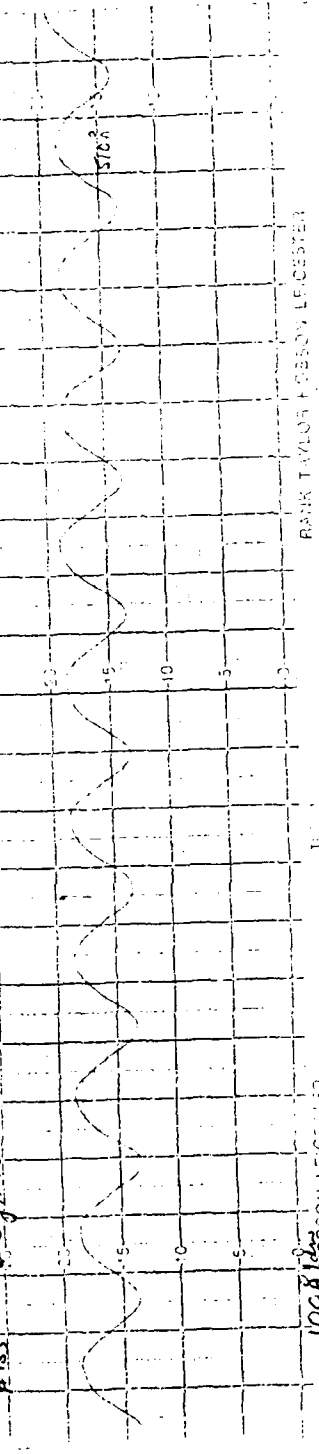
1. STUART, HUTLEY, STEDMAN, App Opt 15, 2618 (1976).
2. AOYAGI and NAMBA, JPN JOURN, App Phys 15, 721 (1976).
3. MATSUI et al, JPN JOURN App Phys 19, 3, pp L126-L128 (1980).
4. JOHNSON, L F, App Optics 18, 15, pp 2559-74 (1979).

14.000

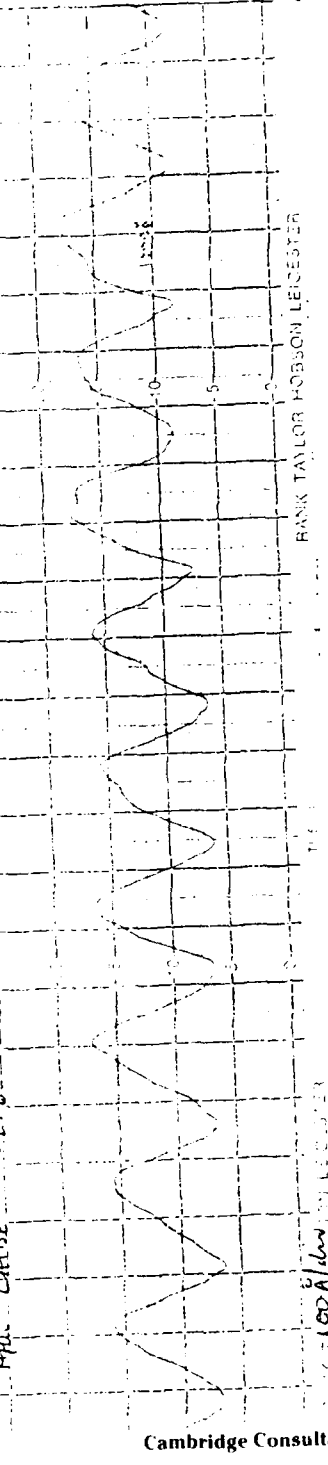
No. 1

#155 6CC g/mms graining 14.000-17 14.000-17

#181 6.00 g/mm PAUL CELLIST MADE IN ENGLAND 14.000-17 1:2



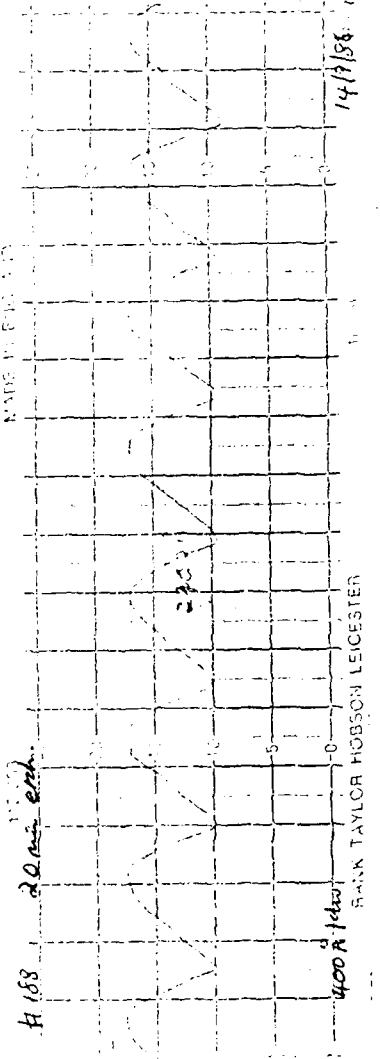
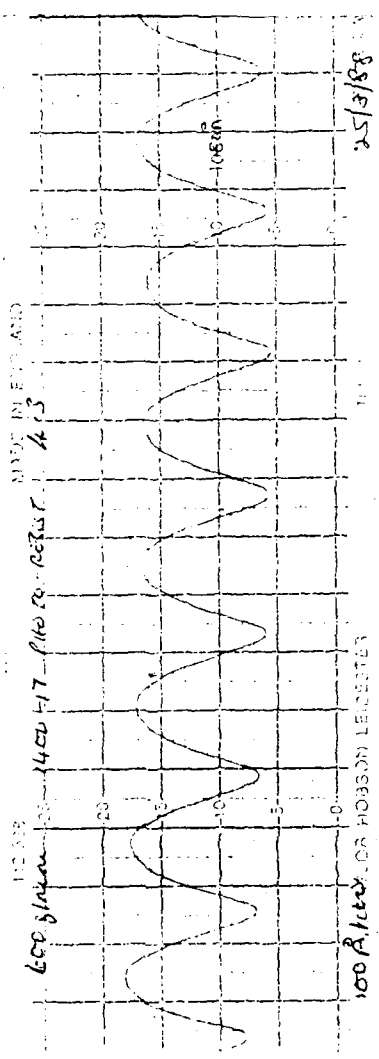
AHL OMBÉ 102 F6 FURTEN JANGIE 64 MADE IN ENGLAND

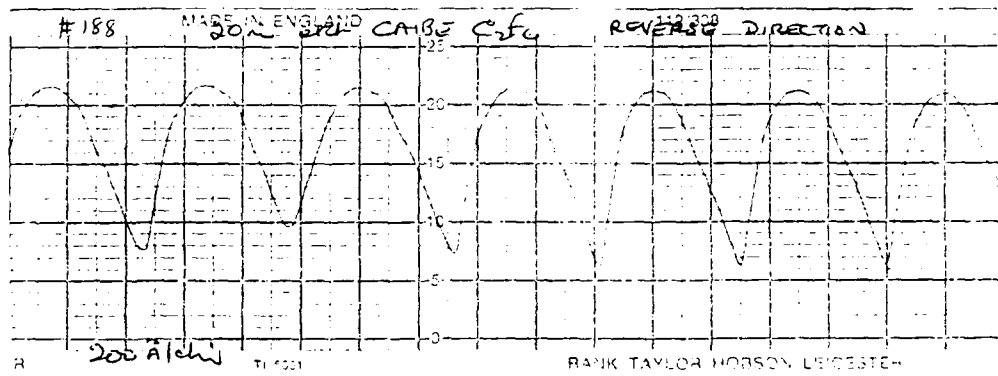
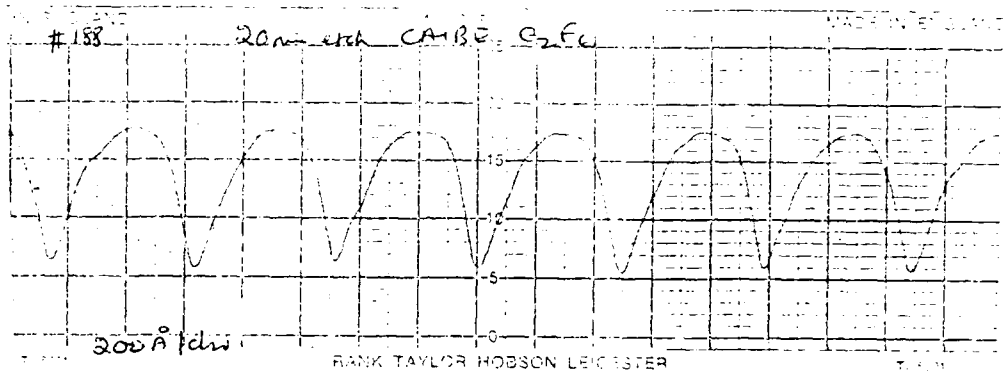


Cambridge Consultants Ltd

Nu -

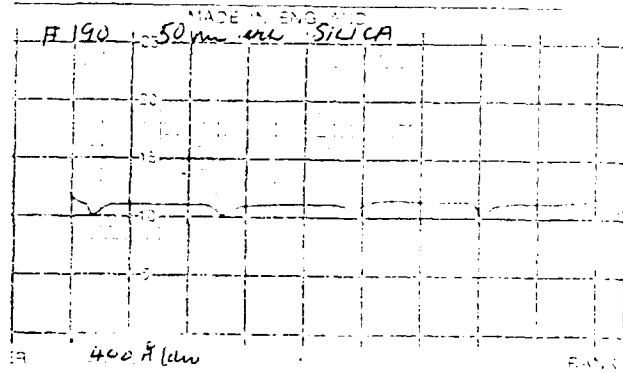
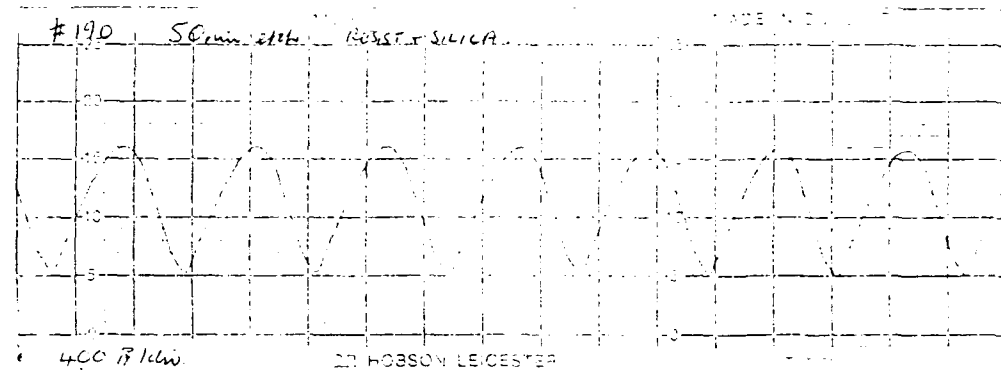
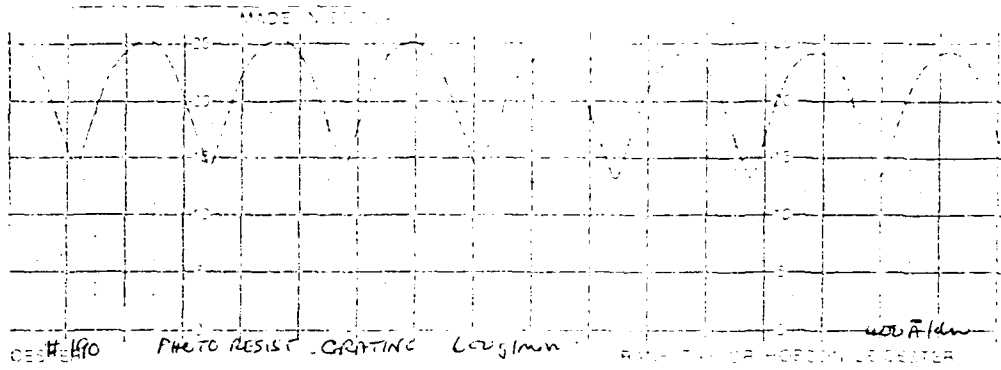
H 168

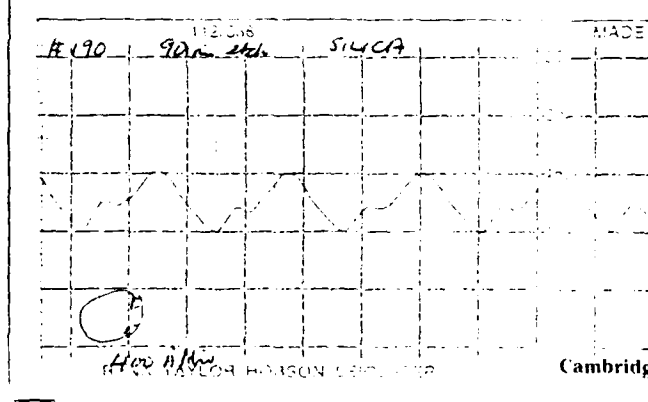
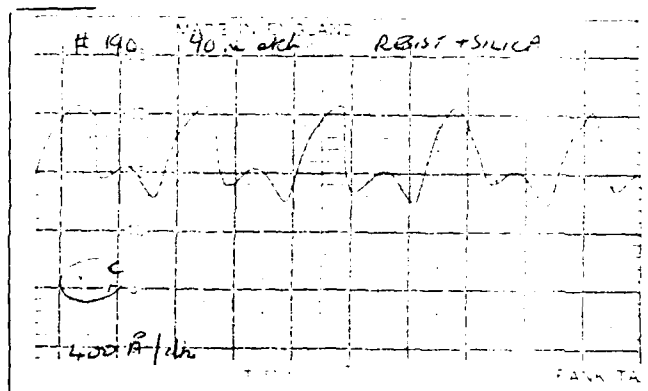
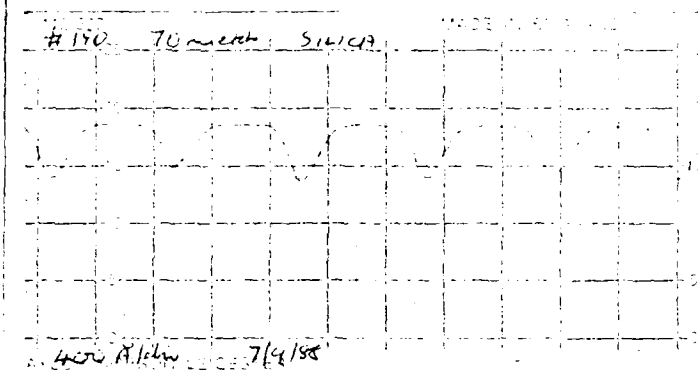
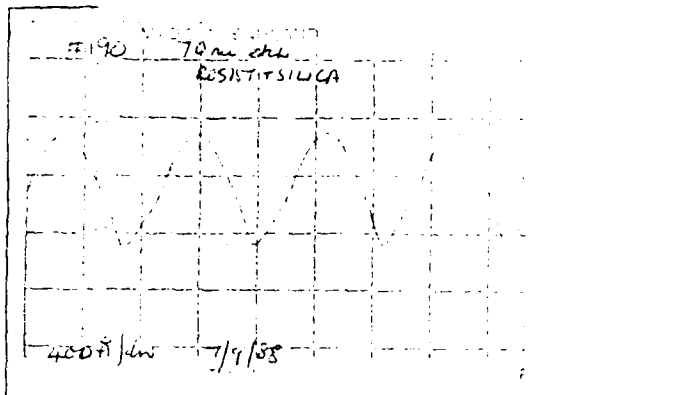


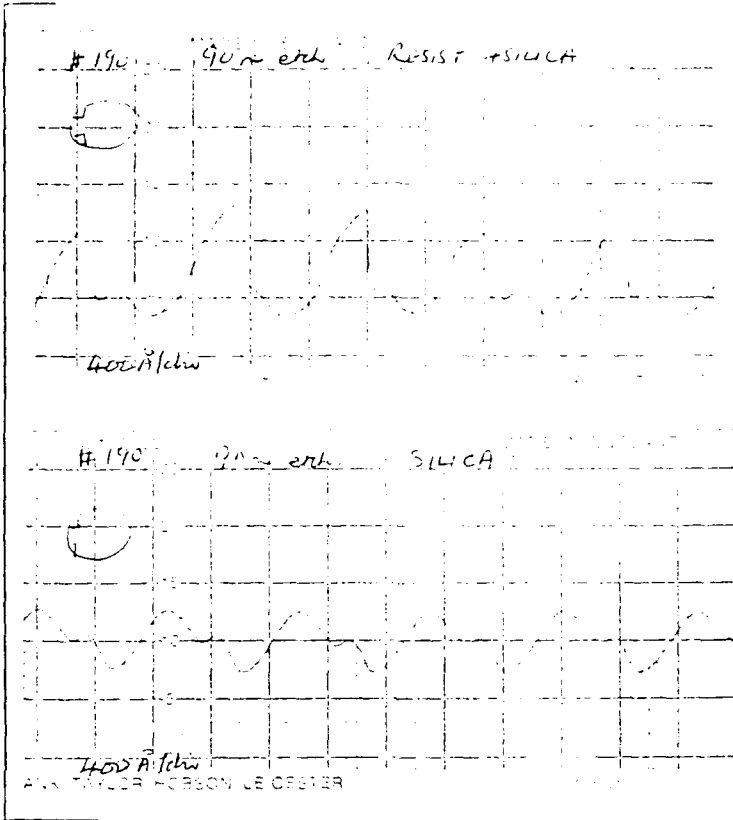


NO. 3.

#190 400 Å







REVERSE DIRECTION  
OF TRAVEL OF  
SUBSTRATE WITH  
RESPECT TO  
TALYFER STY

NO. 4

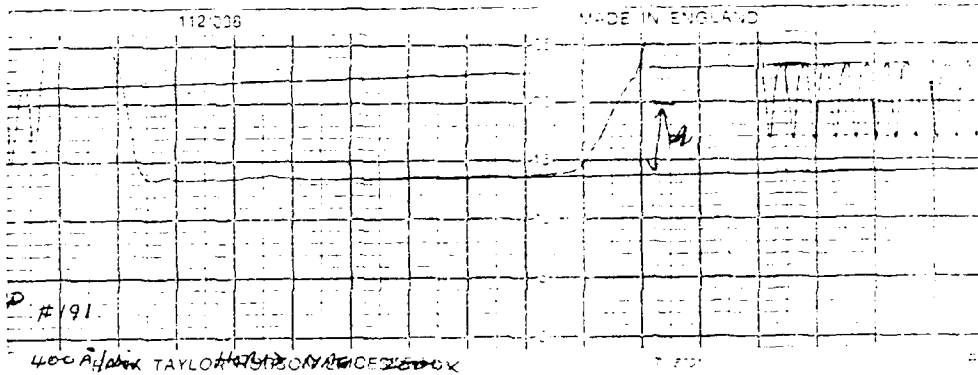
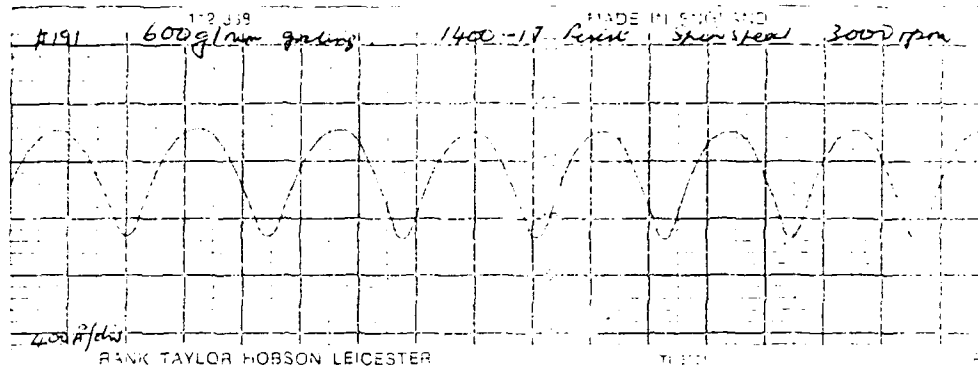


Photo record grinding

Peak to peak amplitude 3720 Å

Measurement of total depth of wave. The depth from 2nd to 4th order  
 horizontal zero two feet from the center line left of grating. Assume  
 beam position of stylus over grating is correct.

Depth from zero pos of grating to zero  $k = 2400 \text{ Å}$

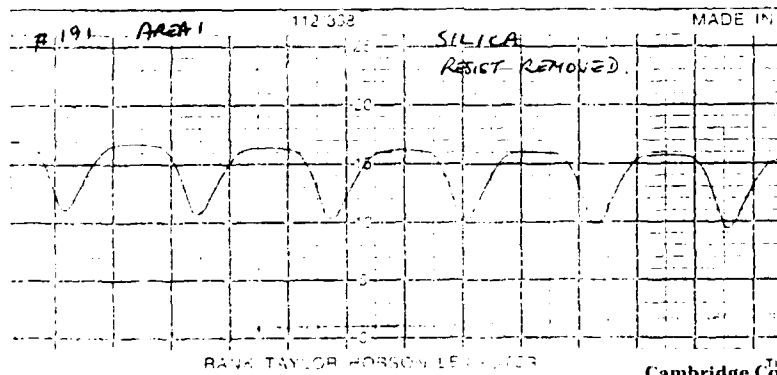
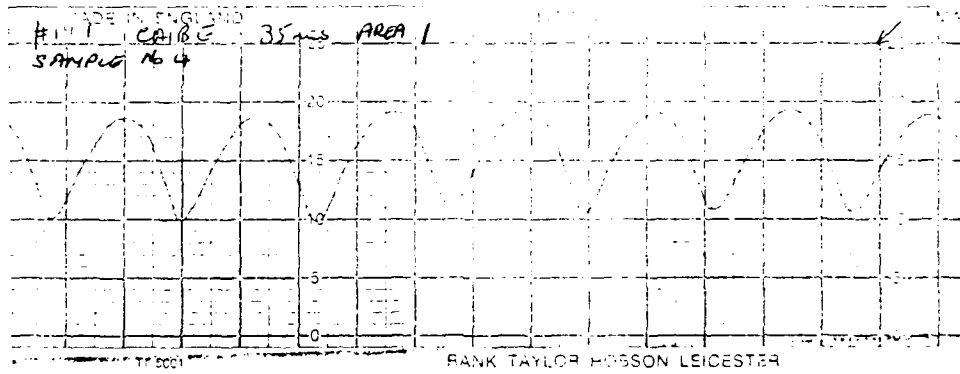
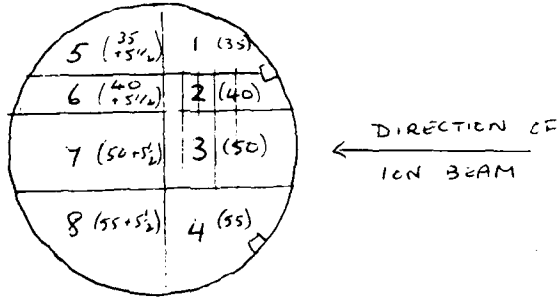
Zero left of zero  $2400 + \frac{27}{2} \times 2 = 4200 \text{ Å}$

Depth of wave below zero  $4200 - 3720 = 480 \text{ Å}$

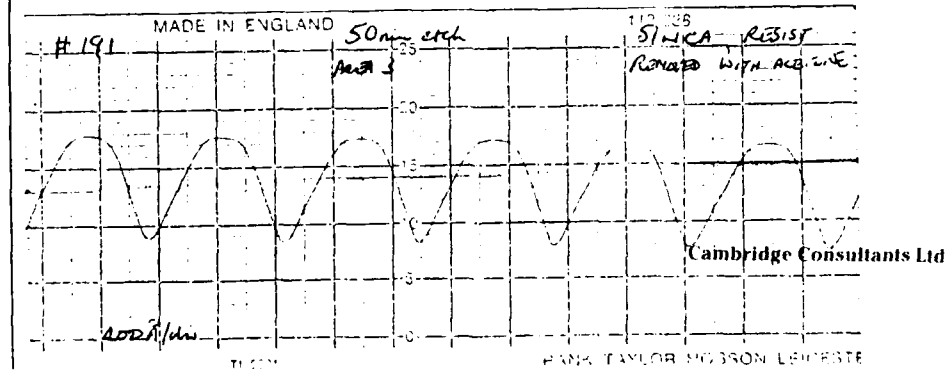
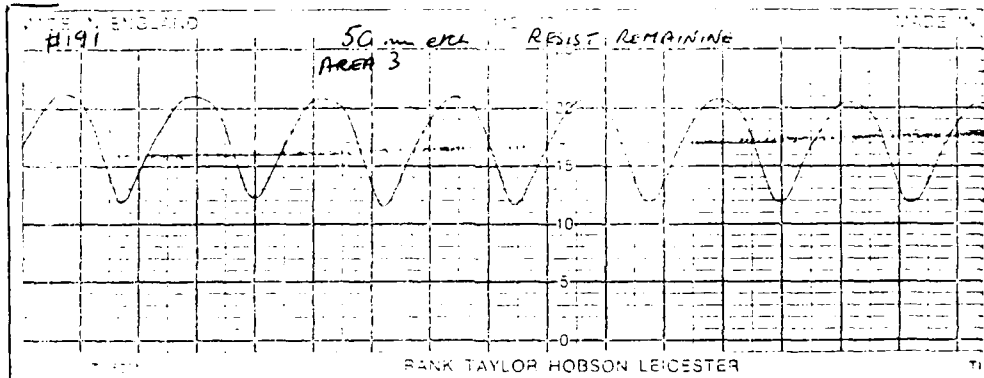
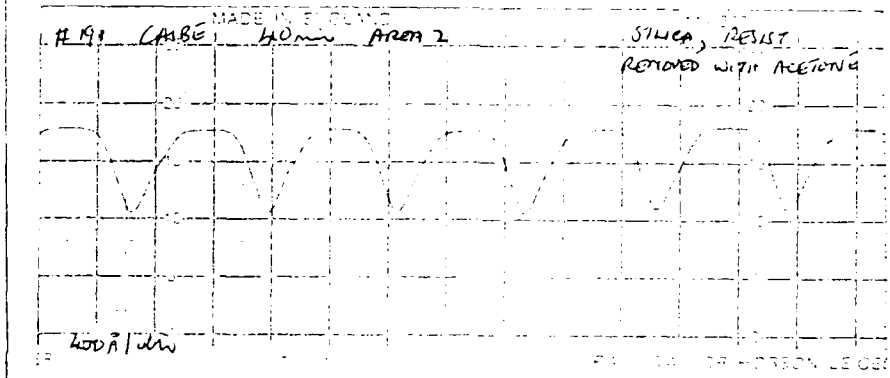
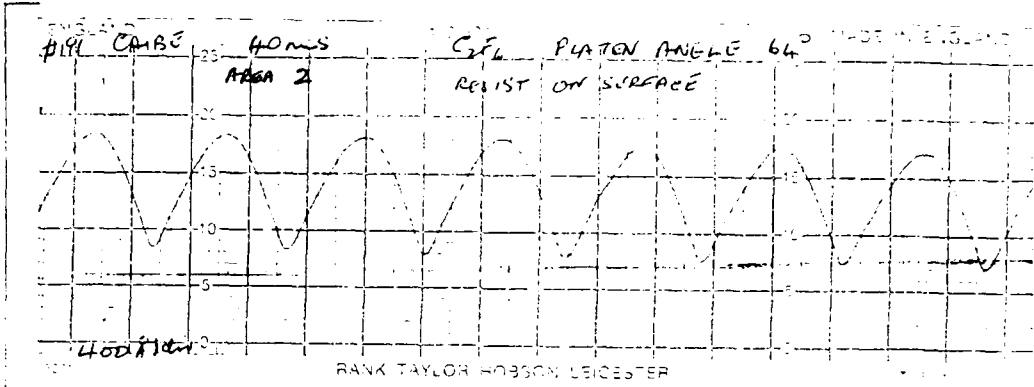
#191 600 g/min SIMULATED CONTINUE

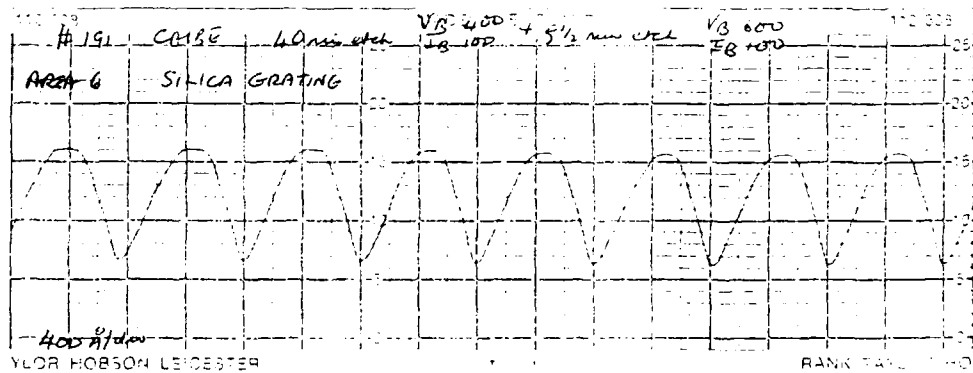
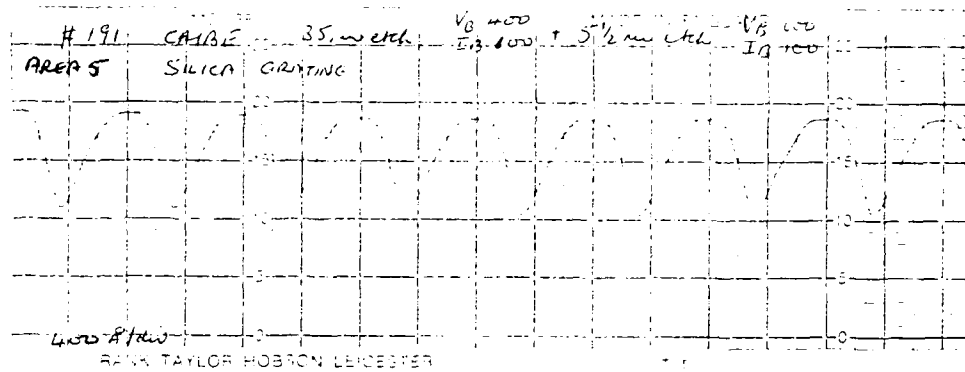
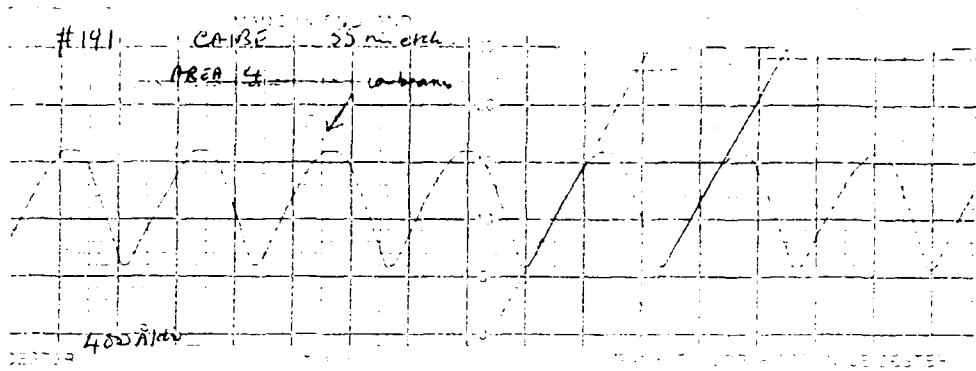
CAIBE C<sub>2</sub>F<sub>6</sub> PLASMA ANGLE 64°

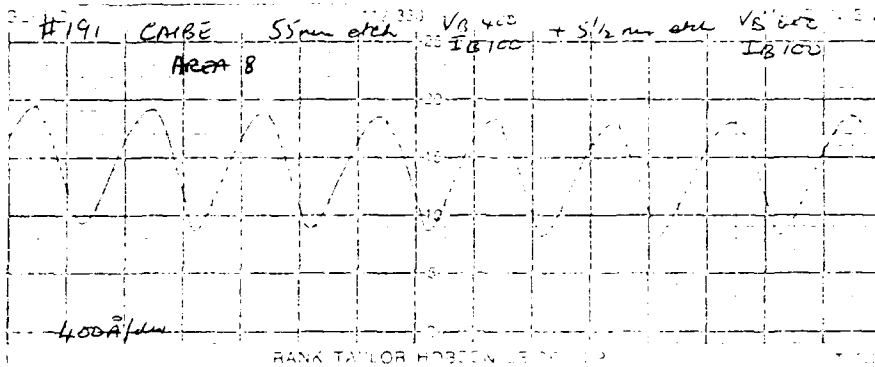
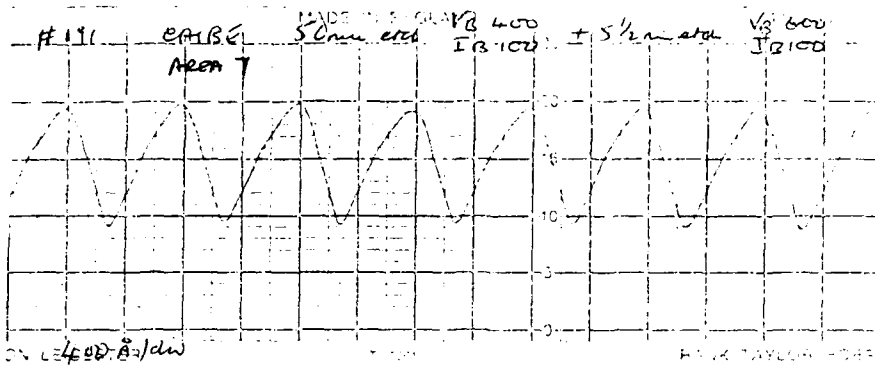
SAMPLE NO 4.



Cambridge Consultants Ltd







APPENDIX C: Grating Specifications

C3086-FR-001a

Cambridge Consultants Ltd

GRATING  
NUMBER : C3086/01

Grating type : Sinusoidal transmission

Frequency :  $600\text{mm}^{-1}$

Substrate size : 30mm diameter

Grating material : photoresist (Shipley Microposit 1400-17)

Grating index : 1.64 at 633nm

Substrate material : synthetic fused silica (Spectrosil-B)

Substrate index : 1.46 at 633nm

Zero-order  
transmission : 4.5% at 633nm

Groove amplitude a'  
(peak-to-peak) : 755nm (estimated)

GRATING  
NUMBER

:C3086/03

Grating type : Sinusoidal transmission

Frequency :  $600\text{mm}^{-1}$

Substrate size : 30mm diameter

Grating material : photoresist (Shipley Microposit 1400-17)

Grating index : 1.64 at 633nm

Substrate material : synthetic fused silica (Spectrosil-B)

Substrate index : 1.46 at 633nm

Zero-order  
transmission : 8.0% at 633nm

Groove amplitude a'  
(peak-to-peak) : 650nm (estimated)

GRATING  
NUMBER : C3086/05

Grating type : etched transmission (quasi-sinusoidal)

Frequency :  $600\text{mm}^{-1}$

Substrate size : 5mm x 5mm (approx)

Grating material : synthetic fused silica (Spectrosil-B)

Grating index : 1.46 at 633nm

Substrate material : n/a

Substrate index : n/a

Zero-order  
transmission : 45.6% at 633nm  
64.1% at 870nm

Groove amplitude a'  
(peak-to-peak) : 550nm (estimated)

GRATING  
NUMBER : C3086/10

Grating type : etched transmission (quasi-sinusoidal)

Frequency :  $600\text{mm}^{-1}$

Substrate size : 5mm x 5mm (approx)

Grating material : synthetic fused silica (Spectrosil-B)

Grating index : 1.46 at 633nm

Substrate material : n/a

Substrate index : n/a

Zero-order  
transmission : 15.0% at 458nm  
2.0% at 633nm  
20.8% at 875nm

Groove amplitude a'  
(peak-to-peak) : 870nm (measured)

GRATING  
NUMBER : C3086/14

Grating type : partially-etched triangular/sinusoidal  
transmission

Frequency :  $600\text{mm}^{-1}$

Substrate size : 30mm diameter

Grating material : photoresist on synthetic fused silica

Grating index : n/a

Substrate material : synthetic fused silica (Spectrosil-B)

Substrate index : 1.46 at 633nm

Zero-order  
transmission : 3% at 594nm  
5% at 633nm  
6% at 875nm

Groove amplitude a'  
(peak-to-peak) :  $1.1\mu\text{m}$  (estimated)

GRATING  
NUMBER : C3086/21 (outline specification)

Grating type : etched transmission

Frequency :  $600\text{mm}^{-1}$

Substrate size : 50mm diameter

Grating material : synthetic fused silica (Synsil)

Grating index : 1.46 at 633nm

Substrate material : n/a

Substrate index : n/a

Zero-order  
transmission : < 10% (peripheral region only, estimated)

Groove amplitude a'  
(peak to peak) : 700nm (estimated)